Scalar tachyonic instabilities in gravitational backgrounds: Existence and growth rate

L. Perivolaropoulos[*] and F. Skara[†]

Department of Physics, University of Ioannina, 45110 Ioannina, Greece

(Received 18 September 2020; accepted 14 October 2020; published 24 November 2020)

It is well known that the Klein Gordon (KG) equation $\Box\Phi + m^2\Phi = 0$ has tachyonic unstable modes on large scales ($k^2 < |m|^2$) for $m^2 < m_{cr}^2 = 0$ in a flat Minkowski spacetime with maximum growth rate $\Omega_F(m) = |m|$ achieved at $k = 0$. We investigate these instabilities in a Reissner-Nordström-deSitter (RN-dS) background spacetime with mass M, charge Q, cosmological constant $\Lambda > 0$ and multiple horizons. By solving the KG equation in the range between the event and cosmological horizons, using tortoise coordinates r_*, we identify the bound states of the emerging Schrodinger-like Regge-Wheeler equation corresponding to instabilities. We find that the critical value m_{cr} such that for $m^2 < m_{cr}^2$ bound states and instabilities appear, remains equal to the flat space value $m_{cr} = 0$ for all values of background metric parameters despite the locally negative nature of the Regge-Wheeler potential for $m = 0$. However, the growth rate Ω of tachyonic instabilities for $m^2 < 0$ gets significantly reduced compared to the flat case for all parameter values of the background metric ($\Omega(Q/M, M^2\Lambda, mM) < |m|$). This increased lifetime of tachyonic instabilities is maximal in the case of a near extreme Schwarzschild-deSitter (SdS) black hole where $Q = 0$ and the cosmological horizon is nearly equal to the event horizon ($\xi \equiv 9M^2\Lambda \simeq 1$). The physical reason for this delay of instability growth appears to be the existence of a cosmological horizon that tends to narrow the negative range of the Regge-Wheeler potential in tortoise coordinates.

DOI: 10.1103/PhysRevD.102.104034

I. INTRODUCTION

Scalar fields are used to describe a wide range of degrees of freedom in a diverse set of physical systems in particle physics (e.g., the Higgs field and other symmetry breaking scalar fields [1]), cosmology (e.g., the inflaton [2] and the quintessence field [3]), gravitational theories (e.g., scalar field hair on black holes [4] or modified gravity scalar degrees of freedom like $f(R)$ theories [5–16] or scalar tensor theories [17]), condensed matter (e.g., the Bose-Eistein scalar field condensate [18]) etc.

The dynamical evolution of a scalar field in a classical system is determined by three main factors

(i) The form of its Lagrangian density and especially the scalar field potential $V(\phi)$ which may be e.g., of the form $V(\phi) = m^2\phi^2$ for a simple massive scalar field or of a symmetry breaking form $V(\phi) = \frac{\lambda}{4}(\phi^2 - \eta^2)^2$ where η is the scale of symmetry breaking.

(ii) The form of the background spacetime which may be for example flat Minkowski, cosmological Friedmann-Robertson-Walker (FRW), Schwarzschild etc.

(iii) The boundary/initial conditions used for the solution of the resulting dynamical scalar field equation emerging from the above two factors.

The simplest Lagrangian density describing the evolution of a scalar field is that corresponding to a free massive scalar which is of the form

$$\mathcal{L} = \frac{1}{2}\partial_\mu\Phi\partial^\mu\Phi - m^2\Phi^2 \tag{1.1}$$

leading to the Klein-Gordon equation [19]

$$\Box\Phi + m^2\Phi = 0. \tag{1.2}$$

In flat Minkowski space this equation may be written as

$$\ddot{\Phi} - \nabla^2\Phi = -m^2\Phi. \tag{1.3}$$

Its solutions are propagating waves of the form

$$\Phi(\vec{r}, t) = A(\vec{k})e^{i(\omega t - \vec{k}\,\vec{r})} + B(\vec{k})e^{-i(\omega t - \vec{k}\,\vec{r})} \tag{1.4}$$

with dispersion relation

$$\omega^2 = k^2 + m^2. \tag{1.5}$$

[*]leandros@uoi.gr
[†]f.skara@uoi.gr

For $m^2 > 0$ we have well behaved propagating waves. However, for $m^2 < 0$ we have

$$\omega = \pm\sqrt{k^2 - |m|^2} \tag{1.6}$$

and exponentially growing tachyonic instabilities develop on large scales ($k < |m|$) where $\mathrm{Im}(\omega) \neq 0$ [20]. In the context of a spontaneous symmetry breaking potential, these instabilities usually imply the presence of a broken symmetry and the transition of the scalar field to a new stable (or metastable) vacuum. However, in the context of a potential that is unbounded from below they may also imply that the theory is unphysical and should be ruled out. This argument has lead to disfavor of a wide range of theories which involve scalar fields with negative m^2 including a wide range of massive Brans-Dicke (BD) theories and $f(R)$ theories where such tachyonic instabilities are also known as Dolgov-Kawasaki-Faraoni (DKF) instabilities [21,22] (see also [23–28]). For example a massive BD scalar field has an action of the form[1] [29–33]

$$S = \frac{1}{16\pi G}\int d^4x\sqrt{-g}\left[\Phi R - \frac{\omega}{\Phi}g^{\mu\nu}\partial_\mu\Phi\partial_\nu\Phi - m^2(\Phi-\Phi_0)^2\right]. \tag{1.7}$$

In this theory (using finite boundary conditions at infinity) a small point mass M located at the origin creates a scalar field and metric configurations of the form

$$\Phi = \Phi_0 + \varphi \tag{1.8}$$

$$g_{\mu\nu} = \eta_{\mu\nu} + h_{\mu\nu} \tag{1.9}$$

where

$$\varphi = \frac{2GM}{(2\omega+3)r}e^{-\bar{m}(\omega)r} \tag{1.10}$$

$$h_{00} = \frac{2GM}{\Phi_0 r}\left(1 + \frac{1}{2\omega+3}e^{-\bar{m}(\omega)r}\right) \tag{1.11}$$

$$h_{ij} = \frac{2GM}{\Phi_0 r}\delta_{ij}\left(1 - \frac{1}{2\omega+3}e^{-\bar{m}(\omega)r}\right) \tag{1.12}$$

with $\bar{m}(\omega) = \sqrt{\frac{2\Phi_0 m^2}{2\omega+3}}$ (Φ_0 is dimensionless) [31].

This h_{00} metric perturbation corresponds to an effective Newton's constant that has a Yukawa correction of the form

$$G_{\mathrm{eff}} = \frac{G}{\Phi_0}\left(1 + \frac{1}{2\omega+3}e^{-\bar{m}(\omega)r}\right). \tag{1.13}$$

[1]The BD parameter ω should not be confused with angular frequency ω used above.

This Yukawa correction is decaying exponentially for $m^2 > 0$ and is observationally/experimentally viable either for large values of $\omega > 40000$ [34] (so that the amplitude of the Newtonian correction is small) or for large values of the scalar field mass m (so that the Newtonian correction decays fast) [31].

For $m^2 < 0$ it is easy to show that the corresponding G_{eff} is spatially oscillating with wavelength $\lambda \simeq \frac{2\pi}{\bar{m}}$

$$G_{\mathrm{eff}} = \frac{G}{\Phi_0}\left(1 + \frac{1}{2\omega+3}\cos\left(\bar{m}(\omega)r + \theta\right)\right) \tag{1.14}$$

where θ is an arbitrary constant. For spatial oscillations of G_{eff} with wavelength less that sub-mm scales ($m \gtrsim 10^{-3}$ eV ($\lambda \lesssim 1$ mm) [35,36]) these spatial oscillations of G_{eff} would have hardly any observational/experimental effects with current experiments/observations despite of the fact that there is no Newtonian limit as $m^2 \to 0^-$ [35,37]. This is due to the local spatial cancellation of the spatially oscillating force correction. However, the main problem with $m^2 < 0$ are tachyonic instabilities [38–41].

It is easy to show that perturbations of the BD scalar Eq. (1.10) obey in flat space a KG equation of the form

$$\ddot{\delta\varphi} - \nabla^2\delta\varphi + m^2\delta\varphi = 0 \tag{1.15}$$

which for $m^2 < 0$ implies the presence of exponentially growing with time tachyonic instabilities for large scales [35]. Thus, this theory with $m^2 < 0$ is only viable if the unstable scales are pushed beyond the cosmological horizon $\sim H_0^{-1}$ which corresponds to scalar field mass $|m| < 10^{-33}$ eV similar to a quintessence scalar field mass. Such spatially oscillating modes have a cosmological horizon scale wavelength and have no observable effects on small scale gravity experiments.

In the case of $f(R)$ theories which may be shown to be equivalent to BD theories with no kinetic term ($\omega = 0$) [42–46] a similar instability occurs. For example the $f(R)$ theory of the form (Starobinsky model [47])

$$f(R) = R + \frac{1}{6m^2}R^2 \tag{1.16}$$

is easily shown to be equivalent to the BD theory with action [35,45,48–52]

$$S_{\mathrm{BD}} = \frac{1}{16\pi G}\int d^4x\sqrt{-g}\left[\Phi R - \frac{3}{2}m^2(\Phi-1)^2\right] + S_{\mathrm{matter}} \tag{1.17}$$

and therefore has the same tachyonic instabilities as the above mentioned massive BD theory (DKF instability).

The parameter value $|m| \simeq 10^{-3}$ eV with $m^2 < 0$ leads to an oscillating Newton's constant with wavelength about

1 mm. In this case the lifetime of the unstable tachyonic modes in Minkowski spacetime would be about 10^{-11} sec. Thus, even though the mass range $|m| > 10^{-3}$ eV with $m^2 < 0$ leads to oscillating modifications of Newton's constant that are consistent with observations/experiments, in the context of $f(R)$ and BD theories and in a flat space background, this mass range is ruled out due to the predicted tachyonic instabilities. This inconsistency is undesirable in view of recent studies [35,53,54][2] that pointed out the existence of oscillating force signals in short range gravity experiments. It is therefore interesting to investigate if there are physical conditions that can eliminate these tachyonic instabilities or at least drastically change their lifetime.

A crucial assumption used in the derivation of the above tachyonic instability is the existence of a Minkowski background. The following questions therefore emerge:

(i) Do scalar tachyonic instabilities for $m^2 < 0$ persist in the presence of a non-flat background?
(ii) How do the instability lifetime and growth rate change in a curved background?
(iii) What are the parameter values of a background metric required to significantly increase the instability lifetime compared to its value in a Minkowski spacetime?

The main goal of the present analysis is to address these questions. In particular we solve the KG equation in a Reissner-Nordström-deSitter (RN-dS) background metric [58,59] with charge Q, mass M and cosmological constant Λ, in the region between the event horizon and the cosmological horizon with boundary conditions corresponding to a finite scalar field Φ with exponential tachyonic instabilities. Using tortoise coordinates that shift these horizons to $\pm\infty$, the KG equation is reduced to a Schrodinger-like Regge-Wheeler equation whose bound states correspond to instability modes. We find the critical value of m^2 ($m^2_{\rm cr}$) such that for $m^2 < m^2_{\rm cr}$ bound states (instability modes) exist. For the tachyonic unstable modes ($m^2 < m^2_{\rm cr}$) we also find the growth rate of the instabilities (ground state eigenvalues of Regge-Wheeler equation) and compare with the corresponding growth rate in a flat Minkowski background. We also consider special cases of the RN-dS metric including the Schwarzschild metric [60], the deSitter (dS) metric [61–65], the Schwarzschild-deSitter (SdS) metric [66,67] and the Reissner-Nordström (RN) metric [68–70].

In the present analysis we focus on the existence of tachyonic exponentially growing solutions and do not consider propagating waves on the boundary horizons which would lead to calculation of quasinormal modes[3] (QNMs) [84,85] (see Refs. [86–90] for reviews on QNMs of black holes). Such investigation of QNMs has been performed in previous studies in Schwarzschild black hole [91–93], in SdS background for $m = 0$ [94–97], for $m^2 > 0$ in RN-dS background [98–101] and in Kerr-deSitter background [102–107] where a different type of instability was observed in the context of scalar field wave scattering. This instability is connected with the phenomenon of superradiance [108–117] in which a reflected wave has larger amplitude than the corresponding incident wave. Superradiant instabilities occur in rotating and in charged black holes embedded in a de Sitter space and are based on the extraction of mass and/or rotational or electromagnetic energy from the black hole. This energy is then carried away from the black hole during a scattering process through the propagation of a reflected scalar field wave with amplitude increased compared to the incident scalar field wave. Superradiance would lead to a decrease in black hole energy and increase of the energy of the scalar field causing further enhancement of the instability. Thus, the endpoints of such instability could be the evacuation of matter from the black hole and/or the formation of a novel scalar field configuration around the black hole leading to a phenomenon called "scalarization" and violation of the no-hair theorem, which states that black holes are fully characterized by their mass, charge and angular momentum. A crucial property of spacetimes with superradiant instabilities is the combination of an event horizon with a cosmological de Sitter horizon in four or higher dimensions [118,119]. In this context one of the goals of the present analysis is the identification of the role of this combination of horizons on tachyonic instabilities and the discussion of their possible connection with superradiant instabilities which involve boundary conditions of propagating wave modes.

The structure of this paper is the following: In the next Sec. II we use spherical tortoise coordinates r_* in the context of an instability ansatz, to transform the KG equation to a Schrodinger-like Regge-Wheeler equation for the radial function $u_l(r_*)$ with potential that depends on the angular scale l, the dimesionless parameters $\xi \equiv 9M^2\Lambda$ and $q \equiv Q/M$ defined above as well as the scalar field mass m^2. The existence of unstable modes that are finite at the two horizons, is equivalent with the existence of bound states of this Regge-Wheeler equation. In Sec. III, we solve the Regge-Wheeler equation numerically and identify the range $m^2(q,\xi)$ for which bound states (unstable modes) exist. In the parameter range that remains unstable ($m^2 < m^2_{\rm cr}(q,\xi)$) we find the growth rate Ω of the instabilities. In Sec. IV we discuss the scalar tachyonic instabilities in the limiting cases of pure deSitter and pure Schwarzschild backgrounds. Finally, in Sec. V we conclude and discuss the physical implications of our results. We also discuss possible extensions of this analysis.

In what follows we use Planck units ($G = c = \hbar = 1$) and a metric signature $(+---)$.

[2]For viable theoretical models with spatially oscillating $G_{\rm eff}$ see [55–57].

[3]A semi-analytical method for calculations of QNMs based on the Wentzel-Kramers-Brillouin (WKB) approximation [71,72]. This method was used in a wide range of spacetimes and in a lot of studies (see e.g., [73–83]).

II. KG equation in SdS/RN-dS spacetimes

A. Schwarzschild-de Sitter background

Consider a SdS background spacetime defined by the metric [66]

$$ds^2 = f(r)dt^2 - \frac{1}{f(r)}dr^2 - r^2(d\theta^2 + \sin^2\theta d\phi^2) \quad (2.1)$$

where

$$f(r) = 1 - \frac{2M}{r} - \frac{\Lambda}{3}r^2 \quad (2.2)$$

In such a background the KG equation (1.2) takes the form

$$\frac{1}{f(r)}\frac{\partial^2\Phi}{\partial t^2} - \frac{\partial}{\partial r}f(r)\frac{\partial\Phi}{\partial r} - \frac{2f(r)}{r}\frac{\partial\Phi}{\partial r} - \frac{\Delta_{\theta\phi}\Phi}{r^2} + m^2\Phi = 0 \quad (2.3)$$

with

$$\Delta_{\theta\phi} = \frac{1}{\sin\theta}\frac{\partial}{\partial\theta}\sin\theta\frac{\partial}{\partial\theta} + \frac{1}{\sin^2\theta}\frac{\partial^2}{\partial\phi^2} \quad (2.4)$$

Using now the ansatz

$$\Phi(t, r, \theta, \phi) = \sum_{lm}\frac{\Psi_l(t, r)}{r}\Upsilon_{lm}(\theta, \phi) \quad (2.5)$$

the eigenvalue equation

$$\Delta_{\theta\phi}\Upsilon_{lm}(\theta, \phi) = -l(l+1)\Upsilon_{lm}(\theta, \phi) \quad (2.6)$$

and transforming to tortoise coordinates defined as (see e.g., [120–122])

$$dr_* \equiv \frac{dr}{f(r)} \quad (2.7)$$

the KG equation reduces to

$$\left(\frac{\partial^2}{\partial t^2} - \frac{\partial^2}{\partial r_*^2} + V_l(r)\right)\Psi_l(t, r_*) = 0 \quad (2.8)$$

where $V_l(r)$ is a Regge-Wheeler type potential which when expressed in the original radial coordinate is of the form

$$V_l(r) = f(r)\left(\frac{l(l+1)}{r^2} + \frac{f'(r)}{r}(1 - s) + m^2\right) \quad (2.9)$$

with $s = 0$ (spin of the considered field) for the case of a scalar field. This type of effective potential was first derived for "axial" (vector type) perturbations in the Schwarzschild background by Regge-Wheeler [123]. For "polar"(scalar type) gravitational perturbations the effective potential was first derived by Zerilli [124,125]. As discussed in [126], the Regge-Wheeler-Zerilli formalism is based on the assumption of spherical symmetry.

For the solution of Eq. (2.8) we need to express the Regge-Wheeler potential $V_l(r)$ in tortoise coordinates $V_{*l}(r_*) \equiv V_l(r(r_*))$. Thus we need to evaluate the integral

$$r_* \equiv \int\frac{dr}{f(r)} = \int\frac{dr}{\sqrt{1 - \frac{2M}{r} - \frac{\Lambda}{3}r^2}} \quad (2.10)$$

To evaluate the integral (2.10) we follow [127] (see also [128]) and factorize $f(r)$. Let

$$\xi = 9M^2\Lambda \quad (2.11)$$

For $\xi < 1$ there are three real solutions of $f(r) = 0$. Two of them correspond to the event and cosmological horizons (r_H and r_C) while the third is negative (r_N) and does not correspond to a physical horizon. The three horizon radii are [121,122,127–132]

$$r_H = \frac{2}{\sqrt{\Lambda}}\cos\left[\frac{1}{3}\cos^{-1}(3M\sqrt{\Lambda}) + \frac{\pi}{3}\right] \quad (2.12)$$

$$r_C = \frac{2}{\sqrt{\Lambda}}\cos\left[\frac{1}{3}\cos^{-1}(3M\sqrt{\Lambda}) - \frac{\pi}{3}\right] \quad (2.13)$$

$$r_N = -(r_H + r_C) \quad (2.14)$$

For $\xi = 1$ which corresponds to the Nariai solution [133,134]) we have an extremal SdS spacetime [120,129,135,136]

$$r_H = r_C = \frac{2}{\sqrt{\Lambda}}\cos\frac{\pi}{3} = \frac{1}{\sqrt{\Lambda}} \simeq 10^{26}\ \text{m} \quad (2.15)$$

where in the last equality we have assumed the observed value of $\Lambda = 3H_0^2\Omega_\Lambda$. The surface gravity of the SdS metric at a coordinate radius r_0 is defined as [96,120,121,137]

$$\kappa_0 \equiv \frac{1}{2}\frac{df}{dr}\bigg|_{r=r_0} = \frac{M}{r_0^2} - \frac{1}{3}\Lambda r_0 \quad (2.16)$$

and describes the gravitational acceleration of a test particle at position r_0. Using Eqs. (2.12), (2.13) and (2.14) to factorize $f(r)$ in Eq. (2.10) and the definition (2.16) we may obtain $r_*(r)$ as [96,127]

$$r_* = \int \frac{dr}{\sqrt{1-\frac{2M}{r}-\frac{\Lambda}{3}r^2}} = \frac{1}{2\kappa_H}\ln\left(\frac{r}{r_H}-1\right)+\frac{1}{2\kappa_C}\ln\left(1-\frac{r}{r_C}\right) + \frac{1}{2\kappa_N}\ln\left(1-\frac{r}{r_N}\right) \tag{2.17}$$

where we note that κ_C is negative.

Using now Eqs. (2.9) and (2.17) it is easy to make a parametric plot of $V_{*l}(r_*)$ by plotting pairs of $(r_*(r), V_l(r))$ for $r \in [r_H, r_C]$.

From Eq. (2.17) it is clear that the tortoise coordinates map the event and cosmological horizons to $\pm\infty$

$$r \to r_H \Rightarrow r_* \to -\infty \qquad r \to r_C \Rightarrow r_* \to +\infty. \tag{2.18}$$

The Regge-Wheeler potential $V_{*l}(r_*)$ of Eq. (2.9) has the important property that it vanishes at both infinities ($\pm\infty$). This is easy to see since

$$V(r_H) = V(r_C) = 0 \Rightarrow \qquad V_*(r_* \to -\infty) = V_*(r_* \to +\infty) = 0. \tag{2.19}$$

As shown below, this property leads to a simple asymptotic solution of Eq. (2.8).

At this point we introduce a rescaling of the radial and time coordinates by M ($r/M \to \bar{r}$, $t/M \to \bar{t}$) and use the dimensionless parameters ξ [defined in Eq. (2.11)] and

$$mM \equiv \frac{GMm}{\hbar c}. \tag{2.20}$$

In order to search for scalar field instabilities we also use the following ansatz in Eq. (2.8)

$$\Psi_l(t, r_*) = (C_1 e^{\Omega t} + C_2 e^{-\Omega t}) u_l(r_*). \tag{2.21}$$

This ansatz along with the above rescaling transforms Eq. (2.8) to a Schrodinger-like Regge-Wheeler equation of the form

$$\frac{du_l^2}{dr_*^2} - M^2(\Omega^2 + V_{*l}(r_*))u_l(r_*) = 0 \tag{2.22}$$

where $r_* \in (-\infty, +\infty)$ and

$$M^2 V_{*0}(r(r_*)) = \left(1-\frac{2}{r(r_*)}-\frac{1}{27}\xi r(r_*)^2\right) \times \left(\frac{2}{r(r_*)^3}-\frac{2}{27}\xi + m^2M^2\right). \tag{2.23}$$

In (2.22), (2.23) we have omitted the bar of the rescaled coordinates and in (2.23) we have fixed $l = 0$. Since $V_{*l}(r) > V_{*l=0}$, the most unstable scales are the large angular scales $l = 0$. This behavior is similar to the case of the Minkowski spacetime discussed in the introduction where the scale corresponding to $k = 0$ was the most unstable scale (largest growth rate, smallest lifetime). Thus in what follows we focus on the $l = 0$ modes. If these modes are stable then all scales ($l > 0$) are also stable.

B. Reissner-Nordström-de Sitter background

We now generalize the metric of the previous section by including charge in the black hole metric. The RN-dS spacetime is defined by the metric function [136,138]

$$f(r) = 1-\frac{2M}{r}+\frac{Q^2}{r^2}-\frac{\Lambda}{3}r^2 = 1-\frac{2}{r}+\frac{q^2}{r^2}-\frac{\xi}{27}r^2 \tag{2.24}$$

where ξ is defined in Eq. (2.11), $q \equiv \frac{Q}{M}$ (where Q is the black hole electric charge) and in the second equality we have used the rescaling $r/M \to r$.

The horizons are obtained by solving the equation $f(r) = 0$. For $\xi < 2$ and $q^2 < 9/8$ there are four real solutions [136]. Two of them correspond to the inner (Cauchy) and outer (event) horizons of a RN black hole r_- and $r_+ = r_H$ (with $0 < r_- < r_H$) respectively. The third corresponds to the cosmological horizon r_C (with $r_C > r_H$) while the fourth r_N (with $r_N = -(r_- + r_H + r_C)$) is negative and does not correspond to a physical horizon.

The three horizons coincide at [136]

$$r_- = r_H = r_C = \frac{3}{\sqrt{2\xi}} \tag{2.25}$$

when $\xi = 2$ and $q^2 = 9/8$.

By demanding that two of the physical horizons coincide we set the discriminant of the quartic equation $f(r) = 0$ to zero and obtain the equation [136,139])

$$1-q^2-\xi+\frac{4}{3}\xi q^2-\frac{8}{27}\xi q^4-\frac{16}{729}\xi^2 q^6 = 0 \tag{2.26}$$

which has real solutions for ξ when $0 < q^2 < \frac{9}{8}$. The critical value $\xi_{H,C}$ at which $r_H = r_C$ and the corresponding value $\xi_{-,H}$ at which $r_- = r_H$ may be obtained in terms of q^2 by solving Eq. (2.26) as

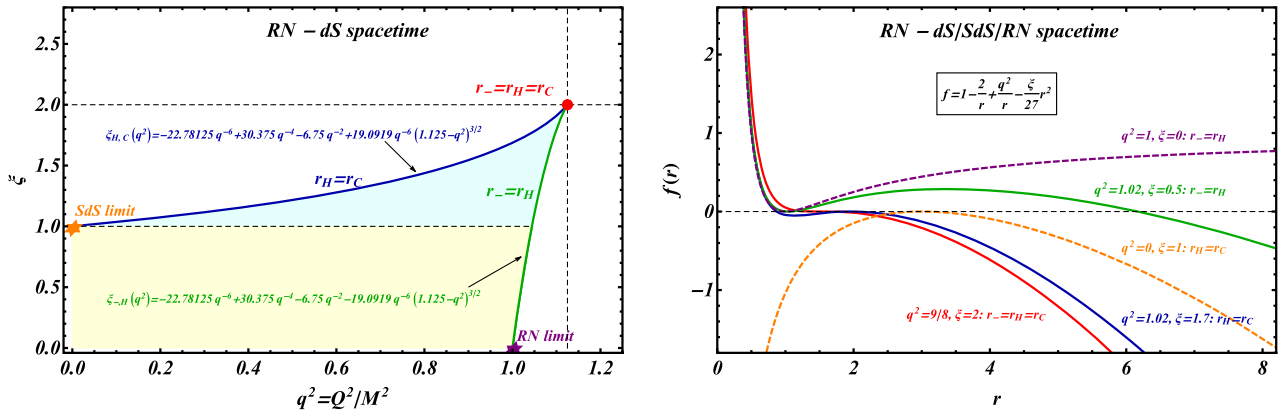

FIG. 1. The critical values $\xi_{H,C}(q^2)$ (with $0 < q^2 < 9/8$) and $\xi_{-,H}(q^2)$ (with $1 < q^2 < 9/8$) as a function of q^2 at which $r_H = r_C$ and $r_- = r_H$ respectively (left panel). The colored shaded regions correspond to the physical corresponding regions of Fig. 6 discussed below. The metric function $f(r)$ as a function of r in the case of the RN-dS/SdS/RN spacetimes for critical value $\xi_{H,C}$ (when event and cosmological horizons coincide) and $\xi_{-,H}$ (when inner Cauchy and outer event horizons coincide) (right panel). The blue, green and red solid curves correspond to RN-dS spacetime while the purple and orange dashed curves correspond to RN and SdS spacetime respectively.

$$\xi_{H,C} = -22.7813q^{-6} + 30.375q^{-4} - 6.75q^{-2} + 19.0919q^{-6}(1.125 - q^2)^{\frac{3}{2}} \tag{2.27}$$

$$\xi_{-,H} = -22.7813q^{-6} + 30.375q^{-4} - 6.75q^{-2} - 19.0919q^{-6}(1.125 - q^2)^{\frac{3}{2}}. \tag{2.28}$$

The first case corresponds to the charged Nariai solution [139]. The critical values $\xi_{H,C}(q^2)$ and $\xi_{-,H}(q^2)$ as a function of q^2 are shown in Fig. 1 (left panel). The critical value $\xi_{H,C}(q^2)$ that leads to a coincidence between the event and cosmological horizons (blue line) varies between 1 (SdS limit, $q = 0$) and 2 (triple horizon coincidence limit, $q^2 = 9/8$). The corresponding form of the function $f(r)$ in these (and in other) limits is shown in Fig. 1 (right panel). The orange line corresponds to the coincidence of the event with the cosmological horizon $r_H = r_C$ in the SdS limit while the blue line shows the coincidence of the same roots of $f(r)$ ($r_H = r_C$) in the general RN-dS case with $q^2 = 1.02$. In both cases the local maximum of $f(r)$ occurs at $f(r) = 0$.

In the case of RN-dS, we study tachyonic instabilities of the neutral massive scalar field perturbations in the event-cosmological horizon region, defined as $r_+ = r_H < r < r_C$ using tortoise coordinates $r_*(r)$ defined as

$$r_* = \int \frac{dr}{\sqrt{1 - \frac{2M}{r} + \frac{Q^2}{r^2} - \frac{\Lambda}{3}r^2}} = \frac{1}{2\kappa_-}\ln\left(\frac{r}{r_-} - 1\right) + \frac{1}{2\kappa_H}\ln\left(\frac{r}{r_H} - 1\right) + \frac{1}{2\kappa_C}\ln\left(1 - \frac{r}{r_C}\right) + \frac{1}{2\kappa_N}\ln\left(1 - \frac{r}{r_N}\right) \tag{2.29}$$

with κ_i ($i = -, H, C$) the surface gravity for the horizon $r = r_i$

$$\kappa_i \equiv \frac{1}{2}\frac{df}{dr}|_{r=r_i} = \frac{M}{r_i^2} - \frac{Q^2}{r_i^3} - \frac{1}{3}\Lambda r_i \tag{2.30}$$

where we note that $\kappa_- < 0$ and $\kappa_C < 0$. It is easy to see that the tortoise coordinates $r_*(r)$ shift the horizons r_H and r_C to $\pm\infty$.

The values of the inner (Cauchy) and outer (event) horizon in the case of RN background ($\Lambda = 0$) for $Q < M$ are (see e.g., [140])

$$r_\pm = M \pm \sqrt{M^2 - Q^2}. \tag{2.31}$$

In the case of RN-dS spacetime a rescaling of the radial and time coordinates by M ($r/M \to r$, $t/M \to t$) and the introduction of the dimensionless parameters ξ [defined in Eq. (2.11)], $q = Q/M$ and mM [defined in Eq. (2.20)] lead to the Schrodinger-like equation (2.22) with maximum scale ($l = 0$) generalized Regge-Wheeler potential of the form

$$M^2 V_{*0}(r(r_*)) = \left(1 - \frac{2}{r(r_*)} + \frac{q^2}{r(r_*)^2} - \frac{1}{27}\xi r(r_*)^2\right) \times \left(\frac{2}{r(r_*)^3} - \frac{2q^2}{r(r_*)^4} - \frac{2}{27}\xi + m^2M^2\right) \tag{2.32}$$

with $r_* \in (-\infty, +\infty)$.

III. NUMERICAL SOLUTION: PARAMETER REGION FOR INSTABILITY, GROWTH RATE

The questions we want to address in this section are the following:

(i) What is the critical value $m_{\rm cr}(q,\xi)^2$ such that for $m^2 > m^2_{\rm cr}$ Eq. (2.22) with a real Ω^2 has no bound state solutions (no instabilities) respecting the physically acceptable boundary conditions that correspond to finite field values at the two horizons ($r_* \to \pm\infty$)?

(ii) What is the growth rate $\Omega(q,\xi,m^2M^2)$ of tachyonic instabilities ($m^2 < m^2_{\rm cr}$) and how does this growth rate compare with the corresponding growth rate in a flat Minkowski spacetime?

We thus solve the Schrodinger-like Regge-Wheeler equation (2.22) and for fixed values of q and ξ we start from a low negative m^2 and identify the ground state solution. Then we increase the value of m^2 until there are no bound states (instability modes) with physically acceptable boundary conditions. At the critical value $m^2 = m^2_{\rm cr}$ there will only be a zero mode solution with eigenvalue $\Omega = 0$ (infinite lifetime mode). Such a mode may be interpreted as a scalar hair zero mode. As discussed in the Introduction, in Minkowski space ($M = \Lambda = Q = 0$), we have $m_{\rm cr} = 0$. *Does this value of $m_{\rm cr}$ change in RN-dS or in SdS spacetimes?*

To address this question we must first find the required "physical boundary conditions." We demand that the physically acceptable solution should be finite on the two horizons i.e.,

$$u_0(r_* \to \infty) < +\infty$$
$$u_0(r_* \to -\infty) < +\infty. \tag{3.1}$$

Since $V_{*0}(r_*)$ goes exponentially fast to 0 for $r_* \to \pm\infty$, we conclude that the general asymptotic solution of Eq. (2.22) is

$$u_0(r_* \to \pm\infty) = Ae^{\Omega r_*} + Be^{-\Omega r_*}. \tag{3.2}$$

For finiteness we demand

$$u_0(r_* \to +\infty) = Be^{-\Omega r_*} \tag{3.3}$$

$$u_0(r_* \to -\infty) = Ae^{\Omega r_*}. \tag{3.4}$$

These imply

$$u_0{}'(r_* \to +\infty) = -\Omega Be^{-\Omega r_*} \tag{3.5}$$

$$u_0{}'(r_* \to -\infty) = \Omega Ae^{\Omega r_*} \tag{3.6}$$

where we can rescale $u_0(r_*)$ such that $A = 1$. These boundary conditions leading to instability may be associated with bound states ($\Omega^2 > 0$, $\Omega \in \mathbb{R}$) of the Schrodinger-like equation (2.22) with effective Regge-Wheeler potential $V_{*0}(r_*)$ (see Eq. (2.23) for SdS spacetime and Eq. (2.32) for RN-dS spacetime). Our search for scalar instabilities ($\Omega^2 > 0$) should be contrasted with the search for the values of QNMs which involves propagating boundary conditions at the horizons. These studies have also indicated the presence of scalar instabilities in a different physical setup (charged massive scalar field in Kerr-Newman black holes with positive m^2 [141]).

The Regge-Wheeler potential $V_{*0}(r_*)$ is mostly accepting bound states for lower values of m^2M^2 and for higher values of Q/M. This is demonstrated in Fig. 2 where we

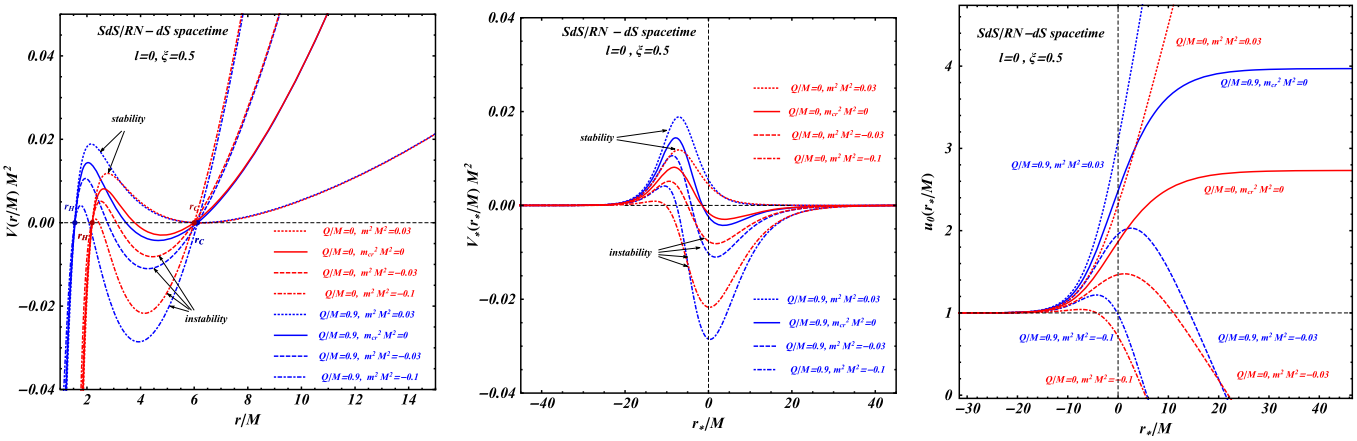

FIG. 2. The m^2M^2 dependent Regge-Wheeler dimensionless potentials VM^2 (left panel) and V_*M^2 (middle panel) as a function of r/M and r_*/M respectively in the cases of the SdS ($Q = 0$) (red curves) and RN-dS ($Q/M = 0.9$) (blue curves) spacetimes for angular scale $l = 0$ and dimensionless parameter fixed to $\xi = 0.5$. The solid curves correspond to the critical value of the scalar field mass $m^2_{\rm cr}M^2 = 0$. The right panel demonstrates the process for identifying the zero eigenvalue eigenstate i.e., setting $\Omega = 0$ in Eq. (2.22) and increasing the dimensionless parameter m^2M^2 until the solution $u_0(r_*/M)$ satisfies both end boundary conditions (3.7)–(3.10) for $\Omega = 0$. This value of m^2M^2 is the critical value for the considered value of ξ. The potential gets deeper and more accepting to bound states (instabilities) as the m^2M^2 gets lower.

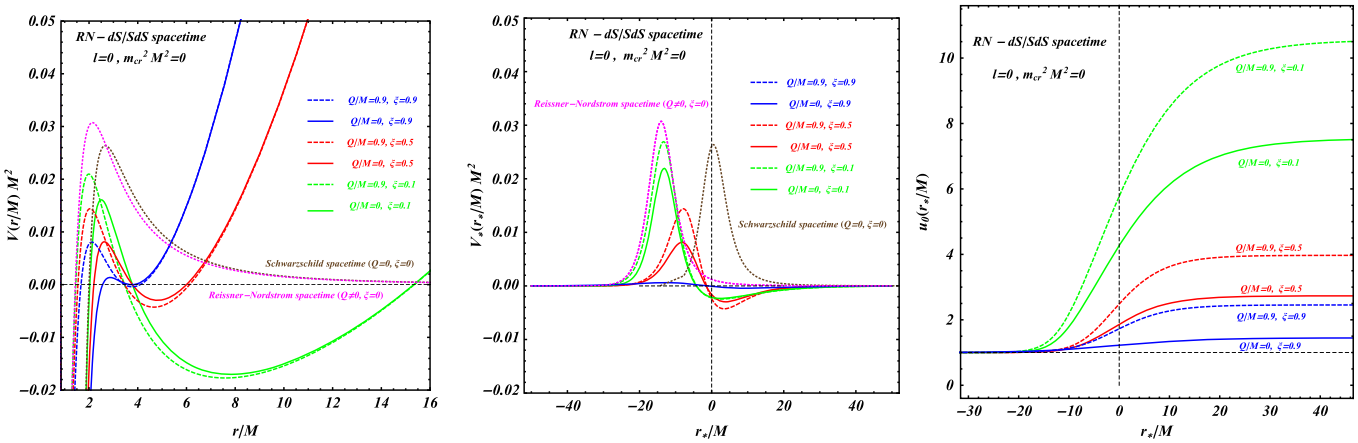

FIG. 3. The ξ dependent Regge-Wheeler dimensionless potentials VM^2 (left panel) and V_*M^2 (middle panel) as a function of r/M and r_*/M respectively in the case of the SdS (solid curves) and RN-dS (dashed curves) spacetimes for angular scale $l=0$ and critical value for $m^2=m_{\rm cr}^2=0$. The radial function $u_0(r_*/M)$ (right panel) which is the radial zero mode solution of Schrodinger-like equation (2.22) with $\Omega=0$ and boundary conditions (3.7) and (3.8) at large negative r_*. For critical value of the scalar field mass $m_{\rm cr}^2M^2=0$ the boundary conditions (3.9) and (3.10) at large positive r_* are satisfied. The brown and purple dotted curves correspond to the pure Schwarzschild ($Q=0$, $\xi=0$) and RN ($Q\neq 0$, $\xi=0$) backgrounds respectively. The potential gets deeper as ξ decreases and Q/M increases. However, since the local maximum of the potential also increases as the potential gets deeper, the critical value $m_{\rm cr}M$ for the existence of bound states remains the same and equal to zero in all cases.

show the form of $V_{*0}(r_*)$ for various values of the dimensionless parameter m^2M^2 in the cases of the SdS ($Q=0$) and RN-dS ($Q/M=0.9$) spacetimes for angular scale $l=0$ and $\xi=0.5$ indicating that as m^2M^2 gets lower and as Q/M gets higher, the minimum of the Regge-Wheeler potential gets deeper and thus it becomes more accepting to the existence of bound states (instabilities). The critical value $m_{\rm cr}(q,\xi)^2$ is such that for $m^2>m_{\rm cr}^2$ there are no bound states (instabilities) respecting the boundary conditions (3.3), (3.4), (3.5), and (3.6).

The critical value $m_{\rm cr}(q,\xi)^2$ is obtained by solving Eq. (2.22) with boundary conditions (3.3), (3.4), (3.5) and (3.6) for a zero eigenvalue $\Omega=0$ corresponding to a borderline unstable mode (zero mode) with infinite lifetime and zero growth rate. For such a zero mode, the boundary conditions (3.3), (3.4), (3.5) and (3.6) become

$$u_0(r_*\to-\infty)=1 \tag{3.7}$$

$$u_0{}'(r_*\to-\infty)=0 \tag{3.8}$$

$$u_0(r_*\to+\infty)=B \tag{3.9}$$

$$u_0{}'(r_*\to+\infty)=0 \tag{3.10}$$

where we have set $A=1$.

In practice we use the shooting method in solving Eq. (2.22) with $\Omega=0$, fixed ξ, q, boundary conditions (3.7), (3.8) at large negative r_* and adjust m^2M^2 until the boundary conditions (3.9) and (3.10) are satisfied (see Fig. 2 right panel). By repeating this process for several values of $q^2\in[0,\frac{9}{8}]$ and $\xi\in[0,\xi_{H,C}(q)]$ we have found $m_{\rm cr}(\xi,q)^2=0$ i.e., the zero mode appears at $m^2=0$ for all parameter values ξ,q where there is a finite distance between the event and the cosmological horizons.

In Fig. 3 we show the form of the Regge-Wheeler potentials $V_0(r/M)$ and $V_{*0}(r_*/M)$ as well as the radial zero mode solution $u_0(r_*/M)$ for the critical value $m_{\rm cr}(q,\xi)=0$ for $\xi=0.1,0.5,0.9$ in the case of the SdS spacetime ($q=0$) and in the case of RN-dS spacetime ($q=0.9$). Notice that in the absence of a cosmological horizon ($\xi=0$, pure Schwarzschild and Reissner-Nordström spacetimes) the Regge-Wheeler potential V_* is positive everywhere for $m=0$ and the absence of bound states is obvious. However, this is not the case for $\xi>0$ which requires numerical solution of the Schrodinger-like equation for the determination of $m_{\rm cr}$.

There is a simple semianalytical way to derive sufficient conditions for instability and for stability and thus test the validity of the numerically obtained form of $m_{\rm cr}^2=0$ for various values of the parameters ξ and q. It is well known that a sufficient condition for the existence of bound states in a Schrodinger equation potential $V_{*0}(r_*)$ is the following sufficient for instability criterion (SIC) [142–144]

$$I_{\rm SIC}=\int_{-\infty}^{+\infty}V_{*0}(r_*)dr_*<0\Longrightarrow$$
$$\int_{r_H}^{r_C}\frac{V_0(r)}{f(r)}dr=\int_{r_H}^{r_C}\left(\frac{l(l+1)}{r^2}+\frac{f'(r)}{r}+m^2\right)_{l=0}dr=$$
$$\int_{r_H}^{r_C}\left(\frac{l(l+1)}{r^2}+\frac{2}{r^3}-\frac{2q^2}{r^4}-\frac{2}{27}\xi+m^2M^2\right)_{l=0}dr<0 \tag{3.11}$$

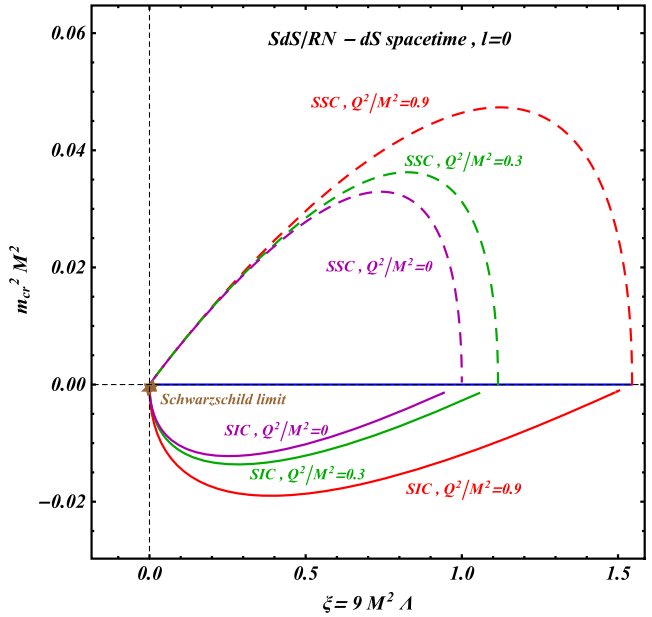

FIG. 4. The critical value of the scalar field mass $m_{\rm cr}^2M^2$ is zero and independent of the dimensionless parameter ξ (with $\xi \in [0, \xi_{H,C}(q)]$) in the case of the SdS and RN-dS spacetime (blue straight line) for $l = 0$. The solid curves show the form of $m_{\rm cr}(q,\xi)^2M^2$ that saturates the Sufficient for Instability Criterion (SIC) Eq. (3.11) while the corresponding dashed curves shows the forms of $m_{\rm cr}(q,\xi)^2M^2$ that saturate the Sufficient for Stability Criterion (SSC) Eq. (3.12) for three values of Q/M. As expected, the exact value of $m_{cr}M = 0$ is between the SIC lines (lower lines) and SSC lines (upper lines) so that none of the criteria is violated (SSC or SIC).

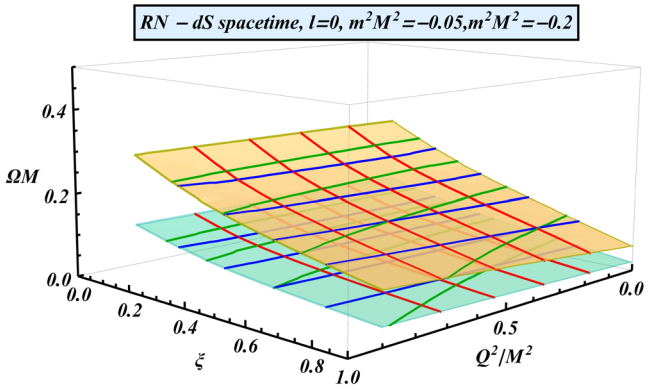

FIG. 5. The dimensionless growth rate of the instability ΩM as a function of the dimensionless parameters ξ and $q^2 = Q^2/M^2$ for scalar field mass $m^2M^2 = -0.05$ (cyan surface) and $m^2M^2 = -0.2$ (yellow surface).

where we have used Eqs. (2.9) and (2.32) for the form of $V_0(r)$ and the dimensionless parameters ξ and q. In addition, a positive definite potential cannot have bound states (negative eigenvalues corresponding to $\Omega^2 > 0$) and thus in such a potential we would only have stable oscillating modes ($\Omega^2 < 0$). Thus a sufficient for stability criterion (SSC) is that the minimum of the Schrodinger potential should be positive i.e.,

$$V_{0,\ \rm min}(r_{\rm min}) > 0. \tag{3.12}$$

Using the SIC and the SSC we have constructed the upper and lower curves in Fig. 4 which correspond to the values of $m(\xi)^2M^2$ that saturate the SSC (upper curves) and SIC (lower curves). Also, using the SSC we find an analytical expression $m^2(\xi)M^2$ for $Q = 0$ (upper curve in Fig. 4 see the Appendix A). Thus, by construction all parameter values below the lower curves satisfy the SIC Eq. (3.11) and must correspond to tachyonic instabilities while all parameter values above the upper curves of Fig. 4 satisfy the SSC Eq. (3.12) and have no instabilities. As expected the precise numerically obtained values of $m_{\rm cr}(\xi)^2 = 0$ are between the SIC and SSC curves so that none of the two sufficient (but not necessary) conditions is violated. Even though the value $m_{\rm cr}(q,\xi) = 0$ for the emergence of tachyonic instabilities is independent of the metric parameters and remains the same in the RN-dS spacetime as in the flat Minkowski spacetime, the growth rate $\Omega(q,\xi,m)$ of tachyonic instabilities ($m^2 < 0$) does have a dependence on the metric parameters. In order to identify this dependence we consider an unstable mode with fixed $m^2 < m_{\rm cr}(q,\xi)^2 = 0$ and given ξ and q, we find the growth rate Ω of the instability by finding the ground state eigenvalue[4] Ω^2 and eigenfunction $u_0(r_*)$ of the Schrodinger-like equation (2.22) which has no nodes and obeys the boundary conditions (3.4)–(3.6), (3.3) and (3.5). We thus construct Fig. 5 which shows the dimensionless growth rate of the instability ΩM as a function of the dimensionless parameters ξ and $q^2 = Q^2/M^2$ for scalar field mass $m^2M^2 = -0.05$ and $m^2M^2 = -0.2$. Clearly, when ξ increases and/or q decreases toward 0, the growth rate of the instability ΩM decreases and as $m^2M^2 \to 0$ we have $\Omega M \to 0$ (the zero mode is reached). In addition to this interesting monotonic behavior of the instability growth rate Ω with respect to the metric parameters, Ω also remains smaller than its flat space value $\Omega_F = |m|$. This is demonstrated in Fig. 6 where we show the dependence of $\frac{\Omega}{\Omega_F}$ on q^2 for various values of ξ for $m^2M^2 = -0.05$ (left panel) and $m^2M^2 = -0.2$ (right panel). We have considered parameter values between the green and blue lines of Fig. 1 where three distinct horizon exist in the RN-dS metric. The following observations can be made based on Figs. 5, 6

(i) The relative growth rate of the tachyonic instabilities $\frac{\Omega}{\Omega_F}$ is a monotonically increasing function of q^2 and a monotonically decreasing function of ξ.

[4]Possible excited states would correspond to lower values of Ω and thus lower growth rate. We thus find the maximum possible growth rate of instabilities for a given set of parameters.

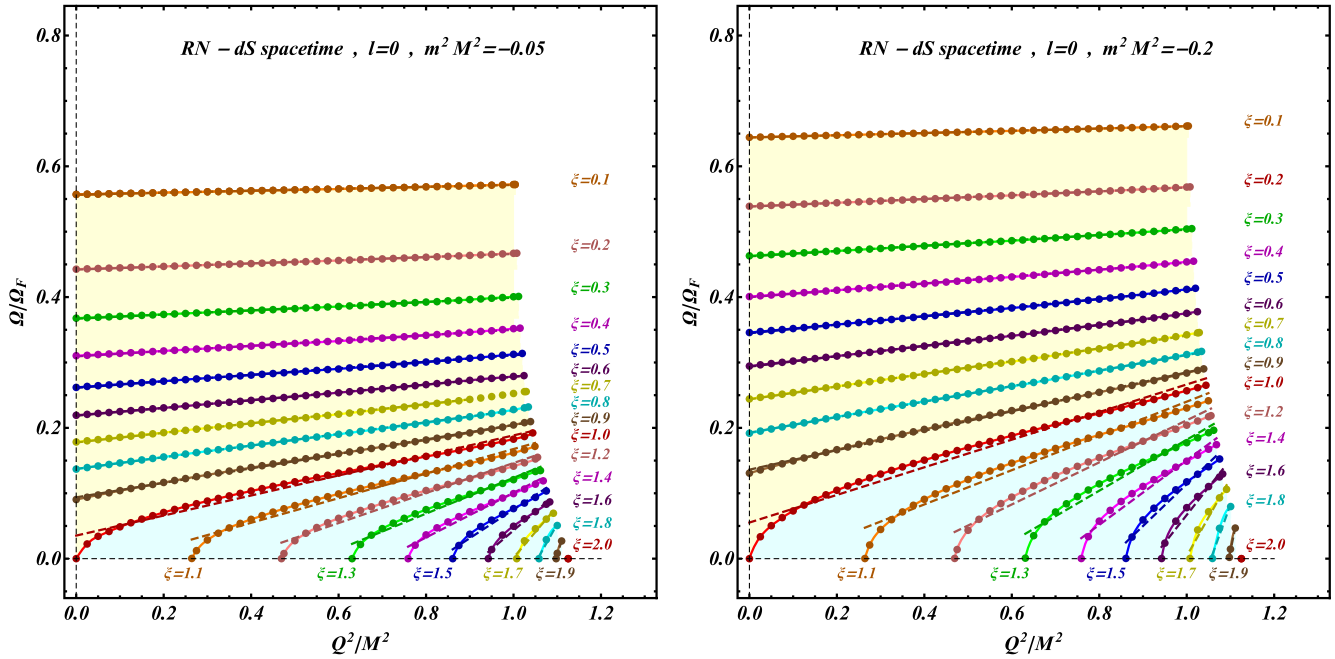

FIG. 6. The ξ dependent relative growth rate of the instability Ω/Ω_F (with Ω_F the growth rate of the instability in flat spacetime) as a function of the dimensionless parameter $q^2 = Q^2/M^2$ for the scalar field mass $m^2M^2 = -0.05$ (left panel) and $m^2M^2 = -0.2$ (right panel). The curves for a given parameter value ξ (with $\xi < 1$) turn out to be straight lines. The range of values of ξ and q is determined by the physically interesting parameter region between the green and blue lines of Fig. 1.The parameter region corresponding to linear behavior of $\Omega(q^2)$ (yellow region) is also shown in Fig. 1.

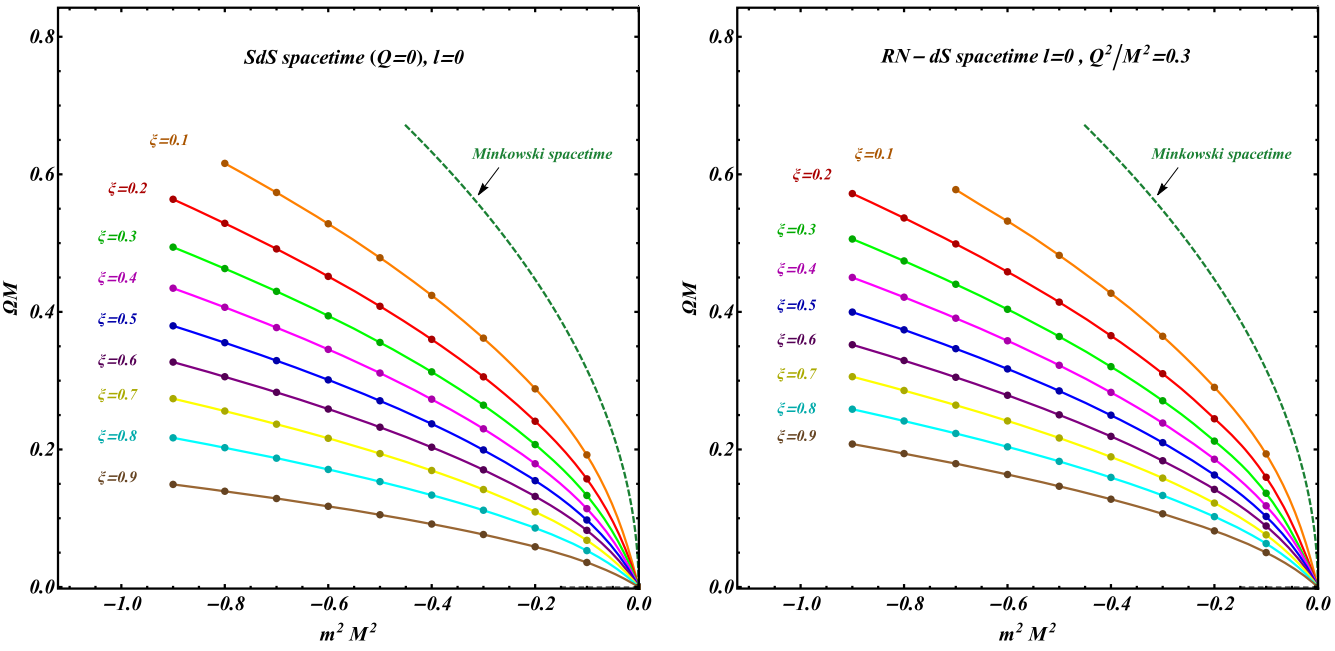

FIG. 7. The ξ dependent dimensionless growth rate of the instability ΩM as a function of the scalar field mass m^2M^2 (with $m(\xi)^2 < m_{\rm cr}(\xi)^2 = 0$) for dimensionless parameters $Q^2/M^2 = 0$ (SdS spacetime) (left panel) and $Q^2/M^2 = 0.3$ (RN-dS spacetime) (right panel). The green dashed curves correspond to $\Omega M(m^2M^2)$ in the case of the Minkowski spacetime. Clearly, for a given field mass, the growth rate is more suppressed in the absence of charge and for higher values of ξ.

(ii) $\frac{\Omega}{\Omega_F}$ is significantly smaller than unity. This reduction implies that background curvature and especially the combination of an event horizon with a cosmological horizon tend to delay the evolution of instabilities.

(iii) There is a linear relation between $\frac{\Omega}{\Omega_F}$ and q^2 for fixed $\xi < 1$. This is evident in both Fig. 6 and in Fig. 5. For example the straight blue lines of Fig. 5 correspond to the dependence of ΩM on q^2 for fixed ξ which are equivalent to the straight lines of Fig. 6. Notice that this linear relation is violated for $\xi > 1$ (see shaded regions in Figs 1, 6).

(iv) The growth rate Ω is a decreasing function of $|m|^2$ which goes to zero as $m^2 \to m^2_{\rm cr} = 0$ where the zero mode develops. This is illustrated in more detail in Fig. 7.

The crucial feature of the RN-dS metric that has lead to the above described trend for delay of instability growth of the tachyonic modes is the combination of the cosmological horizon with an event horizon. This combination, limits the range of negative values of the Regge-Wheeler potential in tortoise coordinates for $m^2 < 0$ and thus makes it less accepting to bound states and instabilities. In the absence of a cosmological horizon the Regge-Wheeler potential in tortoise coordinates would remain negative out to $r_* \to \infty$. This is illustrated in the next section.

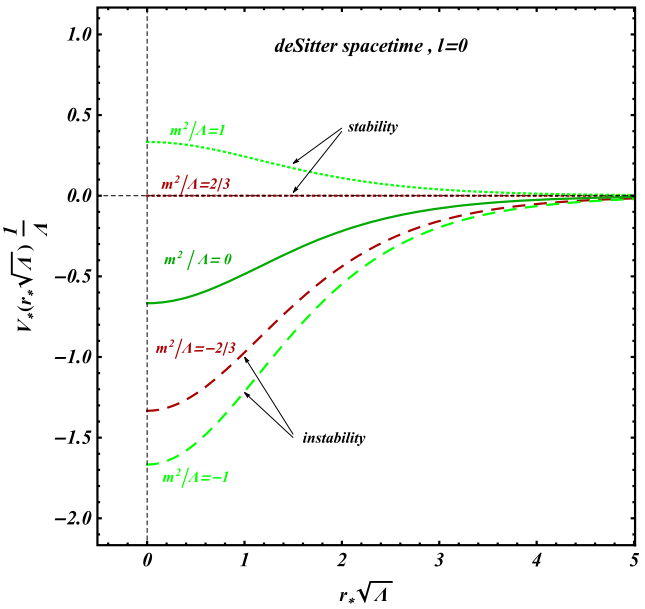

FIG. 8. The m^2/Λ dependent Regge-Wheeler dimensionless potential V_*/Λ as a function of $r_*\sqrt{\Lambda}$ in the case of the deSitter spacetime ($M = 0, \xi = 0$) for angular scale $l = 0$. The green solid curve corresponds to the critical value of the scalar field mass $m^2_{\rm cr}/\Lambda = 0$. The dotted ($m^2/\Lambda > 0$) and dashed ($m^2/\Lambda < 0$) curves correspond to nonexistence of bound states (stabilities) and existence of bound states (instabilities) respectively.

IV. LIMITING CASES WITH A SINGLE HORIZON: PURE DE SITTER AND PURE SCHWARZSCHILD SPACETIMES

We now consider separately the two single horizon limiting cases: pure de Sitter and pure Schwarzschild spacetimes in order to isolate the effects of the cosmological and event horizons.

A. Pure de Sitter background

In the pure de Sitter case ($M = 0$, $Q = 0$), the potential $V_{*0}(r_*)$ is shown in Fig. 8 for various values of m^2/Λ and may be obtained analytically as [145]

$$V_{*0}(r_*) = \frac{m^2 - \frac{2}{3}\Lambda}{\cosh^2 \frac{r_*}{\sqrt{\frac{3}{\Lambda}}}} \simeq^{0<r_*\ll\sqrt{\frac{3}{\Lambda}}} \left(m^2 - \frac{2}{3}\Lambda\right) + \frac{\Lambda}{9}(2\Lambda - 3m^2) r_*^2 + \mathcal{O}(r_*^4) \quad (4.1)$$

After a rescaling $r_*\sqrt{\Lambda} \to r_*$, $m^2/\Lambda \to m^2$ which practically amounts to setting $\Lambda = 1$ it is obvious that the SSC is satisfied for $m^2 > \frac{2}{3}$ which guarantees no instabilities for this range of m^2. Since there is only cosmological horizon in this case, the range of the tortoise coordinate is $r_* \in [0, +\infty]$. For $\Omega = 0$ the Schrodinger-like equation to solve in this case takes the form

$$\frac{du_0^2}{dr_*^2} - \frac{1}{\Lambda} V_*(r_*) u_0(r_*) = 0. \quad (4.2)$$

Since the potential vanishes at $+\infty$ due to the cosmological horizon, the physically interesting (finite) boundary condition at $r_* \longrightarrow +\infty$ is

$$u_0(r_* \to +\infty) = C \quad (4.3)$$

$$u_0{}'(r_* \to +\infty) = 0 \quad (4.4)$$

At the other boundary $r_* \to 0$ we have

$$\frac{dr_*}{dr} = 1 \Rightarrow r_* = r \quad (4.5)$$

and due to Eqs. (2.5) and (2.21) for a finite scalar field at $r = 0$ we must have

$$\Psi_0(r \to 0) = 0 \Rightarrow u_0(r \to 0) = u_0(r_* \to 0) = 0. \quad (4.6)$$

Thus using Eqs. (4.1) and (4.2) it is straightforward to show that

$$u_0(r_* \to 0) = r_* \quad (4.7)$$

where we have used the normalization freedom to set the slope of the linear function to unity. Thus in this case, the physical boundary conditions are

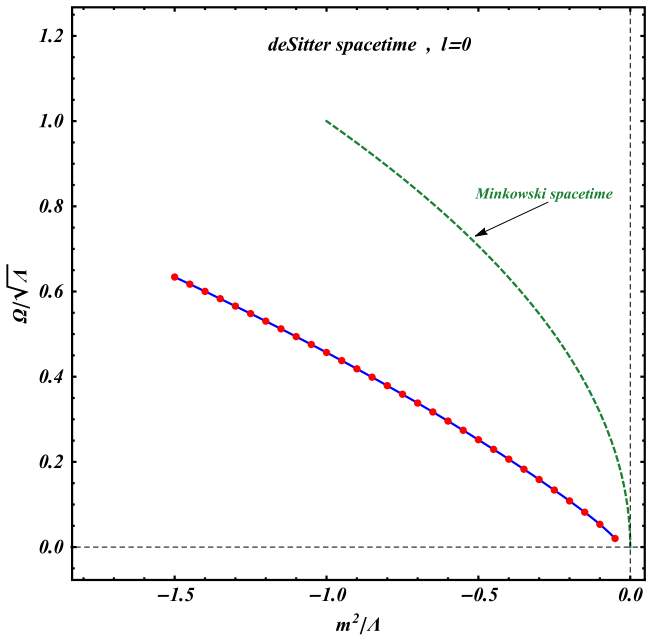

FIG. 9. The dimensionless growth rate of the instability $\Omega/\sqrt{\Lambda}$ as a function of the scalar field mass m^2/Λ (with $m < m_{\rm cr} = 0$) in the case of deSitter spacetime. Clearly $\Omega(m^2/\Lambda) < |m|$ as in the other cases where a cosmological horizon is present.

$$u_0{}'(r_* \to 0) = 1 \tag{4.8}$$

$$u_0(r_* \to 0) = 0 \tag{4.9}$$

$$u_0(r_* \to +\infty) = C \tag{4.10}$$

$$u_0{}'(r_* \to +\infty) = 0. \tag{4.11}$$

Solving Eq. (4.2) corresponding to $\Omega = 0$ from $r_* = 0$ with the boundary conditions (4.8) and (4.9), we obtain (4.10) and (4.11) only for $m_{\rm cr} = 0$. Thus, despite of the negative effective Regge-Wheeler potential in the deSitter background, the tachyonic instabilities develop for the same range of m^2 as in the Minkowski space ($m^2 < 0$). It is straightforward to find the ground state eigenvalue and show that $\Omega(m^2/\Lambda) < |m|$ as in the case of other spacetimes where a cosmological horizon is present (see Fig. 9).

B. Pure Schwarzschild background

In the pure Schwarzschild background ($\Lambda = 0$) we have [146,147]

$$f(r) = 1 - \frac{2M}{r} \tag{4.12}$$

$$V(r) = \left(1 - \frac{2M}{r}\right)\left(\frac{l(l+1)}{r^2} + \frac{2M}{r^3} + m^2\right) \tag{4.13}$$

$$r_*(r) = r + 2M \ln\left(\frac{r}{2M} - 1\right). \tag{4.14}$$

It is easy to see that in both the tortoise and the Schwarzschild coordinates the Regge-Wheeler potential V_{*0} does not vanish asymptotically at $+\infty$. Instead we have (see also Fig. 10)

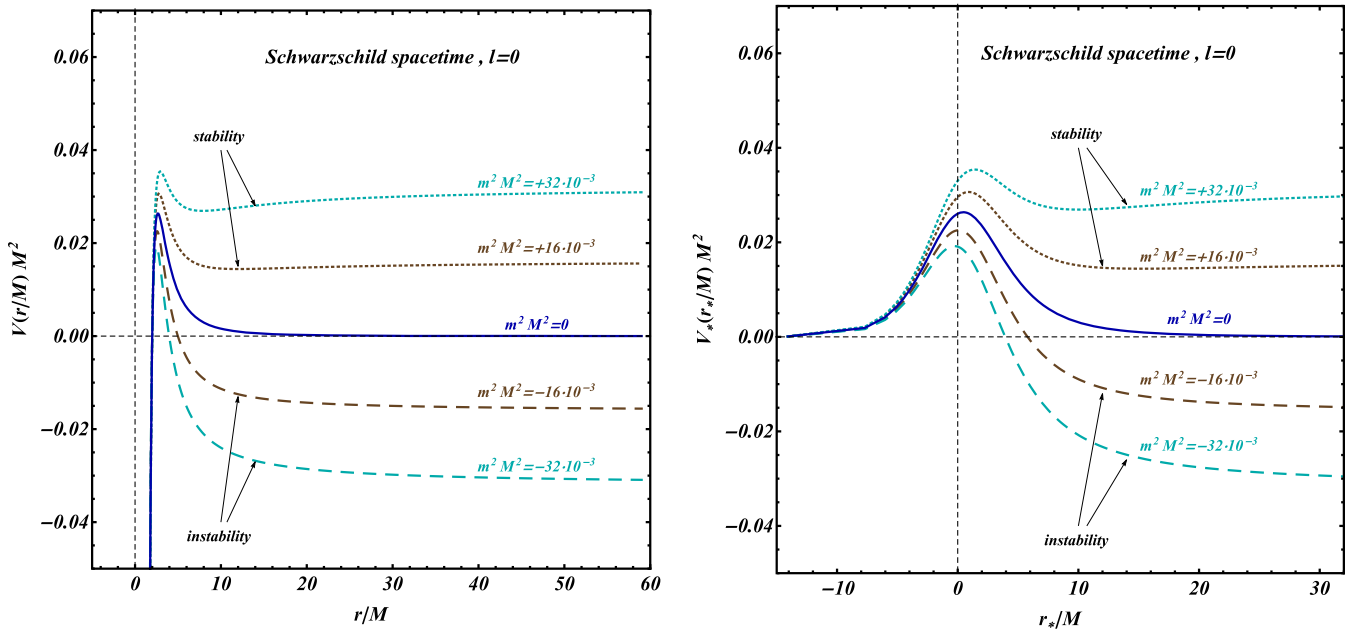

FIG. 10. The m^2M^2 dependent Regge-Wheeler dimensionless potentials VM^2 (left panel) and V_*M^2 (right panel) as a function of r/M and r_*/M respectively in the case of the Schwarzschild spacetime ($\Lambda = 0$, $\xi = 0$) for angular scale $l = 0$. The blue solid curves correspond to the critical value of the scalar field mass $m^2_{\rm cr}M^2 = 0$. The dotted ($m^2M^2 > 0$) and dashed ($m^2M^2 < 0$) curves correspond to nonexistence of bound states (stabilities) and existence of bound states (instabilities) respectively.

$$\lim_{r_*\to+\infty} V_{*0} = m^2. \tag{4.15}$$

This implies that for $m^2 < 0$ the SIC implies instability since

$$\int_{-\infty}^{\infty} V(r_*)dr_* = \int_{r_H}^{\infty} V(r)dr = \int_{r_H}^{\infty}\left(1-\frac{2M}{r}\right)\left(\frac{l(l+1)}{r^2}+\frac{2M}{r^3}+m^2\right)dr = -\infty < 0. \tag{4.16}$$

Therefore for $m^2 < 0$ we have tachyonic instability just as in the Minkowski space. Similarly for $m^2 > 0$ we have $V(r) > 0$ and $V_{*0}(r_*) > 0$ which is the SSC (see also Fig. 10) which secures that we have stability. Thus in the Schwarzchild backround, tachyonic instabilities develop for the same mass parameter range as for the Minkowski background.

In this case, for $m^2 < 0$, the boundary conditions (3.3)–(3.4) become

$$u_0(r_* \to +\infty) = Be^{-i\sqrt{|m|^2-\Omega^2}r_*} \tag{4.17}$$

$$u_0(r_* \to -\infty) = Ae^{\Omega r_*} \tag{4.18}$$

i.e., there are propagating waves toward $+\infty$ even for $m^2 < 0$. There are nonzero solutions satisfying these boundary conditions only for $\Omega \le |m|$. This implies that the maximum growth rate of tachyonic instabilities in this case is the same as in flat space $\Omega = |m|$. This is due to the absence of a cosmological horizon.

V. CONCLUSION, DISCUSSION, OUTLOOK

We have shown that tachyonic scalar instabilities of the KG equation have a slower growth rate in RN-dS/ SdS metric background compared to flat Minkowski space for all values of metric parameters where a cosmological horizons exists. We have also identified the critical value of scalar field mass $m_{\rm cr}^2$ that for $m^2 < m_{\rm cr}^2$ tachyonic instabilities develop and confirmed that $m_{\rm cr} = 0$ as in flat Minkowski spacetime.

The crucial property of the SdS spacetime that allows for this delayed growth of instabilities appears to be the presence of a cosmological horizon that forces the effective Regge-Wheeler potential to vanish at $+\infty$ in tortoise coordinates even for negative scalar field mass m^2. Thus the r_* range where the Regge-Wheeler potential is negative is limited favoring increased eigenvalues and lower growth rate of instabilities.

This stabilizing effect of multiple horizons on tachyonic instabilities may have various interesting implications which include the following

(i) Tachyonic instabilities of $f(R)$ and scalar-tensor theories can get significantly delayed in backgrounds involving cosmological horizons with possible implications for the development of preheating after inflation [20,148–150].
(ii) Symmetry breaking phase transitions in field theory is based on the existence of tachyonic instabilities in a scalar field potential which lead the system toward a new vacuum state with less symmetry. In the context of a RN-dS background the delay of such tachyonic instabilities could have interesting effects in the evolution of phase transitions in the Early Universe with possible interesting observable effects related e.g., to the efficiency of the formation of topological defects [151,152].
(iii) The backreaction effects of the tachyonic instabilities on the gravitational background may lead to superradiance and scalarization effects [115,153] in RN-dS spacetime in the same way that scattering processes lead to similar effects in these spacetimes.
(iv) The consideration of scalar field potentials supporting topological or semilocal defects (e.g., electroweak strings [154]) may lead to interesting new stabilization mechanisms induced by a multihorizon gravitational background.

These implications open up a wide range of extensions of the present analysis. For example interesting extensions include the following:

(i) Consideration of more general background metrics to investigate the existence and growth rate of tachyonic instability modes. Such backgrounds may include Kerr-Newman-deSitter spacetime [153,155–162] or corresponding higher dimension spacetimes, Gödel-like spacetime [163,164] etc.
(ii) Investigate the effects of such delay of instabilities in the Early Universe and in particular during inflation and cosmological phase transitions [165–168] in the context of more general scalar field potentials beyond the KG equation.
(iii) Investigate different types of perturbations (Dirac and gravitational) in multihorizon backgrounds and in the presence of tachyonic modes.
(iv) Consider different types of boundary conditions corresponding to scattering processes (propagating waves at infinity) leading to evaluation of QNMs and scattering amplitudes (superradiance).
(v) Investigate the stability of semilocal and electroweak strings in strongly curved backgrounds including multihorizon metrics.

In conclusion, the interesting nontrivial effects of the gravitational background on the tachyonic scalar instabilities pointed out in the present analysis open up a wide range of new directions in the understanding of the dynamics of scalar fields in curved spacetimes.

The *Mathematica* file used for the numerical analysis and for construction of the figures can be found in [169].

ACKNOWLEDGMENTS

This research is co-financed by Greece and the European Union (European Social Fund - ESF) through the Operational Programme "Human Resources Development, Education and Lifelong Learning 2014-2020" in the context of the project "Scalar fields in Curved Spacetimes: Soliton Solutions, Observational Results and Gravitational Waves" (MIS 5047648). This article has also benefited from COST Action CA15117 (CANTATA), supported by COST (European Cooperation in Science and Technology).

APPENDIX: ANALYTICAL FORM OF SSC CURVES

The above mentioned sufficient for stability criterion (SSC) is that the minimum of the Schrodinger potential should be larger than 0 [see Eq. (3.12)]. Thus by demanding that the minimum of the Schrodinger potential

$$V_{0,\ \min}(r_{\min}) = 0 \tag{A1}$$

we can obtain the analytical form of SSC curves for various values of Q (see Fig. 4). The SSC curve for $Q = 0$ as function of ξ takes the following analytical form

$$m^2(\xi)M^2 = \frac{2(g(\xi)-1)}{9g(\xi)^3} \tag{A2}$$

where

$$g(\xi) = \frac{1}{\left(\sqrt{\xi^4-\xi^3}-\xi^2\right)^{\frac{1}{3}}} + \frac{\left(\sqrt{\xi^4-\xi^3}-\xi^2\right)^{\frac{1}{3}}}{\xi}. \tag{A3}$$

[1] L. Susskind, Dynamics of spontaneous symmetry breaking in the Weinberg-Salam theory, Phys. Rev. D **20**, 2619 (1979).
[2] A. D. Linde, Chaotic inflation, Phys. Lett **129B**, 177 (1983).
[3] I. Zlatev, L.-M. Wang, and P. J. Steinhardt, Quintessence, Cosmic Coincidence, and the Cosmological Constant, Phys. Rev. Lett. **82**, 896 (1999).
[4] C. A. R. Herdeiro and E. Radu, Asymptotically flat black holes with scalar hair: A review, Int. J. Mod. Phys. D **24**, 1542014 (2015).
[5] T. P. Sotiriou and V. Faraoni, f(R) theories of gravity, Rev. Mod. Phys. **82**, 451 (2010).
[6] S. M. Carroll, V. Duvvuri, M. Trodden, and M. S. Turner, Is cosmic speed-up due to new gravitational physics?, Phys. Rev. D **70**, 043528 (2004).
[7] A. De Felice and S. Tsujikawa, f(R) theories, Living Rev. Relativity **13**, 3 (2010).
[8] S. Capozziello, V. F. Cardone, and A. Troisi, Reconciling dark energy models with f(R) theories, Phys. Rev. D **71**, 043503 (2005).
[9] S. Nojiri and S. D. Odintsov, Modified f(R) gravity consistent with realistic cosmology: From matter dominated epoch to dark energy universe, Phys. Rev. D **74**, 086005 (2006).
[10] S. Nojiri and S. D. Odintsov, Introduction to modified gravity and gravitational alternative for dark energy, eConf **C0602061**, 06 (2006).
[11] S. Nojiri and S. D. Odintsov, Modified f(R) gravity unifying R^m inflation with Lambda CDM epoch, Phys. Rev. D **77**, 026007 (2008).
[12] W. Hu and I .Sawicki, Models of f(R) cosmic acceleration that evade solar-system tests, Phys. Rev. D **76**, 064004 (2007).
[13] S. Fay, S. Nesseris, and L. Perivolaropoulos, Can f(R) modified gravity theories mimic a LCDM cosmology?, Phys. Rev. D **76**, 063504 (2007).
[14] S. Capozziello and M. Francaviglia, Extended theories of gravity and their cosmological and astrophysical applications, Gen. Relativ. Gravit. **40**, 357 (2008).
[15] S. Nojiri and S. D. Odintsov, Unified cosmic history in modified gravity: From F(R) theory to Lorentz non-invariant models, Phys. Rep. **505**, 59 (2011).
[16] S. Basilakos, S. Nesseris, and L. Perivolaropoulos, Observational constraints on viable f(R) parametrizations with geometrical and dynamical probes, Phys. Rev. D **87**, 123529 (2013).
[17] B. Boisseau, G. Esposito-Farese, D. Polarski, and A. A. Starobinsky, Reconstruction of a Scalar Tensor Theory of Gravity in an Accelerating Universe, Phys. Rev. Lett. **85**, 2236 (2000).
[18] M. H. Anderson, J. R. Ensher, M. R. Matthews, C. E. Wieman, and E. A. Cornell, Observation of Bose-Einstein condensation in a dilute atomic vapor, Science **269**, 198 (1995).
[19] L. D. Landau and E. M. Lifschits, *The Classical Theory of Fields*, Course of Theoretical Physics, Vol. 2 (Pergamon Press, Oxford, 1975).
[20] G. N. Felder, J. Garcia-Bellido, P. B. Greene, L. Kofman, A. D. Linde, and I. Tkachev, Dynamics of Symmetry Breaking and Tachyonic Preheating, Phys. Rev. Lett. **87**, 011601 (2001).

[21] A. D. Dolgov and M. Kawasaki, Can modified gravity explain accelerated cosmic expansion?, Phys. Lett. B **573**, 1 (2003).
[22] V. Faraoni, Matter instability in modified gravity, Phys. Rev. D **74**, 104017 (2006).
[23] M. E. Soussa and R. P. Woodard, The force of gravity from a Lagrangian containing inverse powers of the Ricci scalar, Gen. Relativ. Gravit. **36**, 855 (2004).
[24] T. Kobayashi and K.-I. Maeda, Relativistic stars in f(R) gravity, and absence thereof, Phys. Rev. D **78**, 064019 (2008).
[25] S. Nojiri and S. D. Odintsov, Modified gravity with negative and positive powers of the curvature: Unification of the inflation and of the cosmic acceleration, Phys. Rev. D **68**, 123512 (2003).
[26] S. Nojiri and S. D. Odintsov, Modified gravity with ln R terms and cosmic acceleration, Gen. Relativ. Gravit. **36**, 1765 (2004).
[27] M. D. Seifert, Stability of spherically symmetric solutions in modified theories of gravity, Phys. Rev. D **76**, 064002 (2007).
[28] I. Sawicki and W. Hu, Stability of cosmological solution in f(R) models of gravity, Phys. Rev. D **75**, 127502 (2007).
[29] C. Brans and R. H. Dicke, Mach's principle and a relativistic theory of gravitation, Phys. Rev. **124**, 925 (1961).
[30] J. Alsing, E. Berti, C. M. Will, and H. Zaglauer, Gravitational radiation from compact binary systems in the massive Brans-Dicke theory of gravity, Phys. Rev. D **85**, 064041 (2012).
[31] L. Perivolaropoulos, PPN parameter gamma and solar system constraints of massive Brans-Dicke theories, Phys. Rev. D **81**, 047501 (2010).
[32] D. F. Torres, Quintessence, superquintessence and observable quantities in Brans-Dicke and nonminimally coupled theories, Phys. Rev. D **66**, 043522 (2002).
[33] S. Sen and T. R. Seshadri, Self-interacting Brans-Dicke cosmology and quintessence, Int. J. Mod. Phys. D **12**, 445 (2003).
[34] C. M. Will, The confrontation between general relativity and experiment, Living Rev. Relativity **17**, 4 (2014).
[35] L. Perivolaropoulos, Submillimeter spatial oscillations of Newton's constant: Theoretical models and laboratory tests, Phys. Rev. D **95**, 084050 (2017).
[36] D. J. Kapner, T. S. Cook, E. G. Adelberger, J. H. Gundlach, B. R. Heckel, C. D. Hoyle, and H. E. Swanson, Tests of the Gravitational Inverse-Square Law Below the Dark-Energy Length Scale, Phys. Rev. Lett. **98**, 021101 (2007).
[37] G. J. Olmo, Post-Newtonian constraints on f(R) cosmologies in metric and Palatini formalism, Phys. Rev. D **72**, 083505 (2005).
[38] S. Capozziello, M. De Laurentis, and V. Faraoni, A Bird's eye view of f(R)-gravity, Open Astron. J. **3**, 49 (2010).
[39] V. Faraoni and N. Lanahan-Tremblay, Comments on Solar system constraints to general f(R) gravity', Phys. Rev. D **77**, 108501 (2008).
[40] S. Nojiri and S. D. Odintsov, Newton law corrections and instabilities in f(R) gravity with the effective cosmological constant epoch, Phys. Lett. B **652**, 343 (2007).
[41] G. Cognola, E. Elizalde, S. Nojiri, S. D. Odintsov, L. Sebastiani, and S. Zerbini, A class of viable modified f(R) gravities describing inflation and the onset of accelerated expansion, Phys. Rev. D **77**, 046009 (2008).
[42] T. Chiba, 1/R gravity and scalar-tensor gravity, Phys. Lett. B **575**, 1 (2003).
[43] P. Teyssandier and P. Tourrenc, The Cauchy problem for the $R + R^2$ theories of gravity without torsion, J. Math. Phys. (N.Y.) **24**, 2793 (1983).
[44] D. Wands, Extended gravity theories and the Einstein-Hilbert action, Classical Quantum Gravity **11**, 269 (1994).
[45] V. Faraoni, Solar system experiments do not yet veto modified gravity models, Phys. Rev. D **74**, 023529 (2006).
[46] S. Capozziello, A. Stabile, and A. Troisi, Comparing scalar-tensor gravity and f(R)-gravity in the Newtonian limit, Phys. Lett. B **686**, 79 (2010).
[47] A. A. Starobinsky, A new type of isotropic cosmological models without singularity, Phys. Lett. **91B**, 99 (1980).
[48] C. P. L. Berry and J. R. Gair, Linearized f(R) gravity: Gravitational radiation and solar system tests, Phys. Rev. D **83**, 104022 (2011); Erratum, Phys. Rev. D **85**, 089906 (2012).
[49] S. Capozziello, A. Stabile, and A. Troisi, A general solution in the Newtonian limit of f(R)- gravity, Mod. Phys. Lett. A **24**, 659 (2009).
[50] S. Capozziello, A. Stabile, and A. Troisi, The Newtonian limit of f(R) gravity, Phys. Rev. D **76**, 104019 (2007).
[51] T. Chiba, T. L. Smith, and A. L. Erickcek, Solar system constraints to general f(R) gravity, Phys. Rev. D **75**, 124014 (2007).
[52] G. J. Olmo, Limit to general relativity in f(R) theories of gravity, Phys. Rev. D **75**, 023511 (2007).
[53] I. Antoniou and L. Perivolaropoulos, Constraints on spatially oscillating sub-mm forces from the stanford optically levitated microsphere experiment data, Phys. Rev. D **96**, 104002 (2017).
[54] L. Perivolaropoulos and L. Kazantzidis, Hints of modified gravity in cosmos and in the lab?, Int. J. Mod. Phys. D **28**, 1942001 (2019).
[55] J. Edholm and A. Conroy, Newtonian potential and geodesic completeness in infinite derivative gravity, Phys. Rev. D **96**, 044012 (2017).
[56] A. Conroy, T. Koivisto, A. Mazumdar, and A. Teimouri, Generalized quadratic curvature, non-local infrared modifications of gravity and Newtonian potentials, Classical Quantum Gravity **32**, 015024 (2015).
[57] J. Edholm, A. S. Koshelev, and A. Mazumdar, Behavior of the Newtonian potential for ghost-free gravity and singularity-free gravity, Phys. Rev. D **94**, 104033 (2016).
[58] K. Lake, Reissner-Nordstrom-de Sitter metric, the third law, and cosmic censorship, Phys. Rev. D **19**, 421 (1979).
[59] H. Laue and M. Weiss, Maximally extended Reissner-Nordstrom manifold with cosmological constant, Phys. Rev. D **16**, 3376 (1977).
[60] K. Schwarzschild, On the gravitational field of a mass point according to Einstein's theory, Sitzungsber. Preuss. Akad. Wiss. Berlin (Math. Phys.) **1916**, 189 (1916), https://ui.adsabs.harvard.edu/abs/1916AbhKP1916..189S/abstract.

[61] W. de Sitter, Einstein's theory of gravitation and its astronomical consequences, First Paper, Mon. Not. R. Astron. Soc. **76**, 699 (1916).
[62] W. de Sitter, Einstein's theory of gravitation and its astronomical consequences, Second Paper, Mon. Not. R. Astron. Soc. **77**, 155 (1916).
[63] W. de Sitter, Einstein's theory of gravitation and its astronomical consequences, Third Paper, Mon. Not. R. Astron. Soc. **78**, 3 (1917).
[64] S. W. Hawking and G. F. R. Ellis, *The Large Scale Structure of Space-Time*, Cambridge Monographs on Mathematical Physics (Cambridge University Press, Cambridge, 2011).
[65] R. Bousso, Adventures in de Sitter space, in *Workshop on Conference on the Future of Theoretical Physics and Cosmology in Honor of Steven Hawking's 60th Birthday* (2002), pp. 539–569, https://ui.adsabs.harvard.edu/abs/2003ftpc.book..539B/abstract.
[66] R. C. Tolman, *Relativity, Thermodynamics, and Cosmology* (Clarendon Press, Oxford, 1934).
[67] H. Stephani, D. Kramer, M. A. H. MacCallum, C. Hoenselaers, and E. Herlt, *Exact Solutions of Einstein's Field Equations*, Cambridge Monographs on Mathematical Physics (Cambridge University Press, Cambridge, England, 2003).
[68] H. Reissner, Über die Eigengravitation des elektrischen Feldes nach der Einsteinschen Theorie, Ann. Phys. (Berlin) **355**, 106 (1916).
[69] G. Nordström, On the energy of the gravitation field in Einstein's theory, K. Ned. Akad. Wet. Proc. B Phys. Sci. **20**, 1238 (1918), https://ui.adsabs.harvard.edu/abs/1918KNAB...20.1238N/abstract.
[70] J. B. Griffiths and J. Podolsky, *Exact Space-Times in Einstein's General Relativity*, Cambridge Monographs on Mathematical Physics (Cambridge University Press, Cambridge, England, 2009).
[71] B. F. Schutz and C. M. Will, Black hole normal modes: A semianalytic approach, Astrophys. J. Lett. **291**, L33 (1985).
[72] S. Iyer and C. M. Will, Black hole normal modes: A WKB approach. 1. Foundations and application of a higher order WKB analysis of potential barrier scattering, Phys. Rev. D **35**, 3621 (1987).
[73] R. A. Konoplya, Quasinormal behavior of the d-dimensional Schwarzschild black hole and higher order WKB approach, Phys. Rev. D **68**, 024018 (2003).
[74] R. A. Konoplya, Quasinormal modes of the electrically charged dilaton black hole, Gen. Relativ. Gravit. **34**, 329 (2002).
[75] R. A. Konoplya, Gravitational quasinormal radiation of higher dimensional black holes, Phys. Rev. D **68**, 124017 (2003).
[76] H. T. Cho, Dirac quasinormal modes in Schwarzschild black hole space-times, Phys. Rev. D **68**, 024003 (2003).
[77] H. Yang, D. A. Nichols, F. Zhang, A. Zimmerman, Z. Zhang, and Y. Chen, Quasinormal-mode spectrum of Kerr black holes and its geometric interpretation, Phys. Rev. D **86**, 104006 (2012).
[78] J. Matyjasek and M. Opala, Quasinormal modes of black holes. The improved semianalytic approach, Phys. Rev. D **96**, 024011 (2017).
[79] Y. Hatsuda, Quasinormal modes of black holes and Borel summation, Phys. Rev. D **101**, 024008 (2020).
[80] S. Devi, R. Roy, and S. Chakrabarti, Quasinormal modes and greybody factors of the novel four dimensional Gauss–Bonnet black holes in asymptotically de Sitter space time: Scalar, electromagnetic and Dirac perturbations, Eur. Phys. J. C **80**, 760 (2020).
[81] M. S. Churilova, Quasinormal modes of the Dirac field in the novel 4D Einstein-Gauss-Bonnet gravity, arXiv:2004.00513.
[82] M. S. Churilova, Quasinormal modes of the test fields in the novel 4D Einstein-Gauss-Bonnet-de Sitter gravity, arXiv:2004.14172.
[83] M. Lagos, P. G. Ferreira, and O. J. Tattersall, Anomalous decay rate of quasinormal modes, Phys. Rev. D **101**, 084018 (2020).
[84] C. V. Vishveshwara, Stability of the schwarzschild metric, Phys. Rev. D **1**, 2870 (1970).
[85] L. A. Edelstein and C. V. Vishveshwara, Differential equations for perturbations on the schwarzschild metric, Phys. Rev. D **1**, 3514 (1970).
[86] K. D. Kokkotas and B. G. Schmidt, Quasinormal modes of stars and black holes, Living Rev. Relativity **2**, 2 (1999).
[87] H.-P. Nollert, Topical review: Quasinormal modes: The characteristic 'sound' of black holes and neutron stars, Classical Quantum Gravity **16**, R159 (1999).
[88] E. Berti, V. Cardoso, and A. O. Starinets, Quasinormal modes of black holes and black branes, Classical Quantum Gravity **26**, 163001 (2009).
[89] V. Ferrari and L. Gualtieri, Quasi-normal modes and gravitational wave astronomy, Gen. Relativ. Gravit. **40**, 945 (2008).
[90] K. Destounis, Dynamical behavior of black-hole spacetimes, Ph.D. thesis, Lisbon, IST, 2019.
[91] S. Hod, Bohr's Correspondence Principle and the Area Spectrum of Quantum Black Holes, Phys. Rev. Lett. **81**, 4293 (1998).
[92] L.-H. Xue, Z.-X. Shen, B. Wang, and R.-K. Su, Numerical simulation of quasinormal modes in time dependent background, Mod. Phys. Lett. A **19**, 239 (2004).
[93] V. Cardoso, J. P. S. Lemos, and S. Yoshida, Quasinormal modes of Schwarzschild black holes in four-dimensions and higher dimensions, Phys. Rev. D **69**, 044004 (2004).
[94] A. Zhidenko, Quasinormal modes of Schwarzschild de Sitter black holes, Classical Quantum Gravity **21**, 273 (2004).
[95] E. Abdalla, C. Molina, and A. Saa, Field propagation in the Schwarzschild-de Sitter black hole, arXiv:gr-qc/0309078.
[96] T. R. Choudhury and T. Padmanabhan, Quasinormal modes in Schwarzschild-deSitter space-time: A simple derivation of the level spacing of the frequencies, Phys. Rev. D **69**, 064033 (2004).
[97] A. M. van den Brink, Approach to the extremal limit of the Schwarzschild-de sitter black hole, Phys. Rev. D **68**, 047501 (2003).
[98] S. Hod, Stability of the extremal Reissner-Nordstroem black hole to charged scalar perturbations, Phys. Lett. B **713**, 505 (2012).
[99] Z. Zhu, S.-J. Zhang, C. E. Pellicer, B. Wang, and E. Abdalla, Stability of Reissner-Nordström black hole in

de Sitter background under charged scalar perturbation, Phys. Rev. D **90**, 044042 (2014); **90**, 049904(A) (2014).
[100] S. Hod, The instability spectra of near-extremal Reissner-Nordström-de Sitter black holes, Phys. Lett. B **786**, 217 (2018); Phys. Lett. B **796**, 256 (2019).
[101] R. A. Konoplya and A. Zhidenko, Charged scalar field instability between the event and cosmological horizons, Phys. Rev. D **90**, 064048 (2014).
[102] S. L. Detweiler, Klein-Gordon equation and rotating black holes, Phys. Rev. D **22**, 2323 (1980).
[103] R. A. Konoplya and A. Zhidenko, Stability and quasinormal modes of the massive scalar field around Kerr black holes, Phys. Rev. D **73**, 124040 (2006).
[104] S. R. Dolan, Instability of the massive Klein-Gordon field on the Kerr spacetime, Phys. Rev. D **76**, 084001 (2007).
[105] V. Cardoso and S. Yoshida, Superradiant instabilities of rotating black branes and strings, J. High Energy Phys. 07 (2005) 009.
[106] H. Witek, V. Cardoso, A. Ishibashi, and U. Sperhake, Superradiant instabilities in astrophysical systems, Phys. Rev. D **87**, 043513 (2013).
[107] H. Okawa, H. Witek, and V. Cardoso, Black holes and fundamental fields in numerical relativity: Initial data construction and evolution of bound states, Phys. Rev. D **89**, 104032 (2014).
[108] J. D. Bekenstein, Extraction of energy and charge from a black hole, Phys. Rev. D **7**, 949 (1973).
[109] T. Damour, N. Deruelle, and R. Ruffini, On quantum resonances in stationary geometries, Lett. Nuovo Cimento **15**, 257 (1976).
[110] R. A. Konoplya and A. Zhidenko, Quasinormal modes of black holes: From astrophysics to string theory, Rev. Mod. Phys. **83**, 793 (2011).
[111] V. Cardoso, Black hole bombs and explosions: From astrophysics to particle physics, Gen. Relativ. Gravit. **45**, 2079 (2013).
[112] Y. Shlapentokh-Rothman, Exponentially growing finite energy solutions for the Klein-Gordon equation on sub-extremal Kerr spacetimes, Commun. Math. Phys. **329**, 859 (2014).
[113] C. A. R. Herdeiro, J. C. Degollado, and H. Freyr Rúnarsson, Rapid growth of superradiant instabilities for charged black holes in a cavity, Phys. Rev. D **88**, 063003 (2013).
[114] C.-Y. Zhang, S.-J. Zhang, and B. Wang, Superradiant instability of Kerr-de Sitter black holes in scalar-tensor theory, J. High Energy Phys. 08 (2014) 011.
[115] R. Brito, V. Cardoso, and P. Pani, *Superradiance: Energy Extraction, Black-Hole Bombs and Implications for Astrophysics and Particle Physics* (Springer, New York, 2015), Vol. 906.
[116] N. Sanchis-Gual, J. C. Degollado, P. J. Montero, J. A. Font, and C. Herdeiro, Explosion and Final State of an Unstable Reissner-Nordström Black Hole, Phys. Rev. Lett. **116**, 141101 (2016).
[117] G. Moschidis, Superradiant instabilities for short-range non-negative potentials on Kerr spacetimes and applications, arXiv:1608.02041.
[118] A. Zhidenko, Linear perturbations of black holes: Stability, quasi-normal modes and tails, Ph.D. thesis, Sao Paulo University, 2009.
[119] K. Destounis, Superradiant instability of charged scalar fields in higher-dimensional Reissner-Nordström-de Sitter black holes, Phys. Rev. D **100**, 044054 (2019).
[120] V. Cardoso and J. P. S. Lemos, Quasinormal modes of the near extremal Schwarzschild-de Sitter black hole, Phys. Rev. D **67**, 084020 (2003).
[121] T. R. Choudhury and T. Padmanabhan, Concept of temperature in multi-horizon spacetimes: Analysis of Schwarzschild-de Sitter metric, Gen. Relativ. Gravit. **39**, 1789 (2007).
[122] B. Toshmatov and Z. Stuchlík, Slowly decaying resonances of massive scalar fields around Schwarzschild-de Sitter black holes, Eur. Phys. J. Plus **132**, 324 (2017).
[123] T. Regge and J. A. Wheeler, Stability of a Schwarzschild singularity, Phys. Rev. **108**, 1063 (1957).
[124] F. J. Zerilli, Gravitational field of a particle falling in a Schwarzschild geometry analyzed in tensor harmonics, Phys. Rev. D **2**, 2141 (1970).
[125] F. J. Zerilli, Effective Potential for Even Parity Regge-Wheeler Gravitational Perturbation Equations, Phys. Rev. Lett. **24**, 737 (1970).
[126] G. G. L. Nashed and S. Capozziello, Charged spherically symmetric black holes in $f(R)$ gravity and their stability analysis, Phys. Rev. D **99**, 104018 (2019).
[127] S. Bhattacharya, Particle creation by de Sitter black holes revisited, Phys. Rev. D **98**, 125013 (2018).
[128] Z. Stuchlík, P. Slany, and J. Kovar, Pseudo-Newtonian and general relativistic barotropic tori in Schwarzschild-de Sitter spacetimes, Classical Quantum Gravity **26**, 215013 (2009).
[129] Z. Stuchlík, The motion of test particles in black-hole backgrounds with non-zero cosmological constant, Bull. Astron. Inst. Czech. **34**, 129 (1983), https://ui.adsabs.harvard.edu/abs/1983BAICz..34..129S/abstract.
[130] G. W. Gibbons and S. W. Hawking, Cosmological event horizons, thermodynamics, and particle creation, Phys. Rev. D **15**, 2738 (1977).
[131] J. Guven and D. Núñez, Schwarzschild-de Sitter space and its perturbations, Phys. Rev. D **42**, 2577 (1990).
[132] A. Ashtekar and B. Krishnan, Dynamical horizons and their properties, Phys. Rev. D **68**, 104030 (2003).
[133] H. Nariai, On some static solutions of Einstein's gravitational field equations in a spherically symmetric case, Sci. Rep. Tohoku Univ. Eighth Ser. **34**, 160 (1950), https://ui.adsabs.harvard.edu/abs/1950SRToh..34..160N/abstract.
[134] R. Bousso and S. W. Hawking, (Anti)evaporation of Schwarzschild-de Sitter black holes, Phys. Rev. D **57**, 2436 (1998).
[135] K. Lake and R. C. Roeder, Effects of a nonvanishing cosmological constant on the spherically symmetric vacuum manifold, Phys. Rev. D **15**, 3513 (1977).
[136] L. J. Romans, Supersymmetric, cold and lukewarm black holes in cosmological Einstein-Maxwell theory, Nucl. Phys. **B383**, 395 (1992).
[137] S. W. Hawking, Particle creation by black holes, Commun. Math. Phys. **43**, 199 (1975); Erratum, Commun. Math. Phys. **46**, 206 (1976).
[138] P. R. Brady, C. M. Chambers, W. Krivan, and P. Laguna, Telling tails in the presence of a cosmological constant, Phys. Rev. D **55**, 7538 (1997).

[139] M. Montero, T.Van Riet, and G. Venken, Festina Lente: EFT constraints from charged black hole evaporation in de Sitter, J. High Energy Phys. 01 (2020) 039.
[140] C. W. Misner, K. S. Thorne, and J. A. Wheeler, *Gravitation* (W. H. Freeman, San Francisco, 1973).
[141] R. A. Konoplya and A. Zhidenko, Massive charged scalar field in the Kerr-Newman background I: Quasinormal modes, late-time tails and stability, Phys. Rev. D **88**, 024054 (2013).
[142] W. F. Buell and B. A. Shadwick, Potentials and bound states, Am. J. Phys. **63**, 256 (1995).
[143] G. Dotti and R. J. Gleiser, Gravitational instability of Einstein-Gauss-Bonnet black holes under tensor mode perturbations, Classical Quantum Gravity **22**, L1 (2005).
[144] Y. S. Myung and D.-C. Zou, Instability of Reissner–Nordström black hole in Einstein-Maxwell-scalar theory, Eur. Phys. J. C **79**, 273 (2019).
[145] D.-P. Du, B. Wang, and R.-K. Su, Quasinormal modes in pure de Sitter space-times, Phys. Rev. D **70**, 064024 (2004).
[146] D. B. Sibandze, R. Goswami, S. D. Maharaj, A. M. Nzioki, and P. K. S. Dunsby, Scattering of Ricci scalar perturbations from Schwarzschild black holes in modified gravity, Eur. Phys. J. C **77**, 364 (2017).
[147] W.-D. Li, Y.-Z. Chen, and W.-S. Dai, Scattering state and bound state of scalar field in Schwarzschild spacetime: Exact solution, Ann. Phys. (Amsterdam) **409**, 167919 (2019).
[148] R. Allahverdi, R. Brandenberger, F.-Y. Cyr-Racine, and A. Mazumdar, Reheating in inflationary cosmology: Theory and applications, Annu. Rev. Nucl. Part. Sci. **60**, 27 (2010).
[149] M. He, R. Jinno, K. Kamada, A. A. Starobinsky, and J. Yokoyama, Occurrence of tachyonic preheating in the mixed Higgs-R^2 model, arXiv:2007.10369.
[150] M. A. Amin, M. P. Hertzberg, D. I. Kaiser, and J. Karouby, Nonperturbative dynamics of reheating after inflation: A review, Int. J. Mod. Phys. D **24**, 1530003 (2015).
[151] J. Ye and R. H. Brandenberger, The formation and evolution of U(1) gauged vortices in an expanding universe, Nucl. Phys. **B346**, 149 (1990).
[152] A. Achucarro, J. Borrill, and A. R Liddle, The Formation Rate of Semilocal Strings, Phys. Rev. Lett. **82**, 3742 (1999).
[153] E. Winstanley, On classical superradiance in Kerr-Newman-anti–de Sitter black holes, Phys. Rev. D **64**, 104010 (2001).
[154] M. James, L. Perivolaropoulos, and T. Vachaspati, Stability of electroweak strings, Phys. Rev. D **46**, R5232 (1992).
[155] B. Carter, Global structure of the Kerr family of gravitational fields, Phys. Rev. **174**, 1559 (1968).
[156] Z. Stuchlik, G. Bao, E. Ostgaard, and S. Hledik, Kerr-Newman-de Sitter black holes with a restricted repulsive barrier of equatorial photon motion, Phys. Rev. D **58**, 084003 (1998).
[157] J. Podolsky and J. B. Griffiths, Accelerating Kerr-Newman black holes in (anti-)de Sitter space-time, Phys. Rev. D **73**, 044018 (2006).
[158] Z. Stuchlik and S. Hledik, Equatorial photon motion in the Kerr-Newman spacetimes with a non-zero cosmological constant, Classical Quantum Gravity **17**, 4541 (2000).
[159] G. V. Kraniotis, Gravitational lensing and frame dragging of light in the Kerr-Newman and the Kerr-Newman-(anti) de Sitter black hole spacetimes, Gen. Relativ. Gravit. **46**, 1818 (2014).
[160] G. V. Kraniotis, The Klein–Gordon–Fock equation in the curved spacetime of the Kerr–Newman (anti) de Sitter black hole, Classical Quantum Gravity **33**, 225011 (2016).
[161] G. V. Kraniotis, The massive Dirac equation in the Kerr-Newman-de Sitter and Kerr-Newman black hole spacetimes, J. Phys. Commun. **3**, 035026 (2019).
[162] G. V. Kraniotis, Gravitational redshift/blueshift of light emitted by geodesic test particles, frame-dragging and pericentre-shift effects, in the Kerr-Newman-de Sitter and Kerr-Newman black hole geometries, arXiv:1912.10320.
[163] R. A. Konoplya, Superluminal neutrinos and the tachyon's stability in the rotating Universe, Phys. Lett. B **706**, 451 (2012).
[164] R. A. Konoplya and A. Zhidenko, Stability of tardyons and tachyons in the rotating and expanding Universe, Phys. Rev. D **86**, 023531 (2012).
[165] T. W. B. Kibble, Topology of cosmic domains and strings, J. Phys. A **9**, 1387 (1976).
[166] W. H. Zurek, Cosmological experiments in superfluid Helium?, Nature (London) **317**, 505 (1985).
[167] A. Rajantie, 'Phase transitions in the early universe' and 'Defect formation', in *COSLAB Workshop on Cosmological Phase Transitions and Topological Defects* (2003), https://ui.adsabs.harvard.edu/abs/2003hep.ph...11262R/abstract.
[168] T. W. B. Kibble, Some implications of a cosmological phase transition, Phys. Rep. **67**, 183 (1980).
[169] http://leandros.physics.uoi.gr/tachyonic-instabilities.zip.